

LANGMUIR PROBE MEASUREMENTS IN THE PLUME OF A PULSED PLASMA
THRUSTER

by

Robert Francis Eckman

A Thesis

Submitted to the Faculty

of the

WORCESTER POLYTECHNIC INSTITUTE

in partial fulfillment of the requirements for the

Degree of Master of Science

in

Mechanical Engineering

February 1999

APPROVED:

Dr. Nikos A. Gatsonis, Advisor

Dr. David J. Olinger, Committee Member

Dr. James C. Hermanson, Committee Member

Eric J. Pencil, NASA Lewis Research Center, Committee Member

Dr. Mark W. Richman, Graduate Committee Representative

Abstract

As new, smaller satellites are built, the need for improved on-board propulsion systems has grown. The pulsed plasma thruster has received attention due to its low power requirements, its simple propellant management, and the success of initial flight tests. Successful integration of PPTs on spacecraft requires the comprehensive evaluation of possible plume-spacecraft interactions. The PPT plume consists of neutrals and ions from the decomposition of the Teflon propellant, material from electrode erosion, as well as electromagnetic fields and optical emissions. To investigate the PPT plume, an on-going program is underway at WPI that combines experimental and computational investigations. Experimental investigation of the PPT plume is challenging due to the unsteady, pulsed as well as the partially ionized character of the plume. In this thesis, a triple Langmuir probe apparatus was designed and used to obtain electron temperature and density measurements in the plume of a PPT. This experimental investigation provides further characterization of the plume, much needed validation data for computational models, and is useful in thruster optimization studies.

The pulsed plasma thruster used in this study is a rectangular geometry laboratory model built at NASA Lewis Research Center for component lifetime tests and plume studies. It is almost identical in size and performance to the LES 8/9 thruster, ablating 26.6 μg of Teflon, producing an impulse bit of 256 $\mu\text{N}\cdot\text{s}$ and a specific impulse of 986 s at 20 J. All experiments were carried out at NASA LeRC Electric Propulsion Laboratory.

The experimental setup included triple Langmuir probes mounted on a moveable probe stand, to collect data over a wide range of locations and operating conditions.

Triple probes have the ability to instantaneously measure electron temperature and density, and have the benefit of being relatively simple to use, compared to other methods used to measure these same properties. The implementation of this measuring technique is discussed in detail, to aid future work that utilizes these devices. Electron temperature and density was measured from up to 45 degrees from the centerline on planes parallel and perpendicular to the thruster electrodes, for thruster energy levels of 5, 20 and 40 J. Radial distances extend from 6 to 20 cm downstream from the Teflon surface. These locations cover the core of the PPT plume, over a range of energy levels that corresponds to proposed mission operating conditions.

Data analysis shows the spatial and temporal variation of the plume. Maximum electron density near the exit of the thruster is 1.6×10^{20} , 1.6×10^{21} , and $1.8 \times 10^{21} \text{ m}^{-3}$ for the 5, 20 and 40 J discharges, respectively. At 20 cm downstream from the Teflon surface, densities are 1×10^{19} , 1.5×10^{20} and 4.2×10^{20} for the 5, 20 and 40 J discharges, respectively. The average electron temperature at maximum density was found to vary between 3.75 and 4.0 eV for the above density measurements at the thruster exit, and 20 cm from the Teflon surface the temperatures are 0.5, 2.5, and 3 eV for the 5, 20 and 40 J discharges. Plume properties show a great degree of angular variation in the perpendicular plane and very little in the parallel plane, most likely due to the rectangular geometry of the PPT electrodes. Simultaneous electron temperature and density traces for a single thruster discharge show that the hottest electrons populate the leading edge of the plume. Analysis between pulses shows a 50% variation in density and a 25% variation in electron temperature. Error analysis estimates that maximum uncertainty in the temperature measurements to be approximately $\pm 0.75 \text{ eV}$ due to noise smoothing,

and the maximum uncertainty in electron density to be $\pm 60\%$, due to assumptions related to the triple probe theory.

In addition, analysis of previously observed slow and fast ion components in the PPT plume was performed. The analysis shows that there is approximately a $3 \mu\text{s}$ difference in creation time between the fast and slow ions, and that this correlates almost exactly with the half period of the oscillations in the thruster discharge current.

Acknowledgements

This work is an extension of my undergraduate project work at WPI. For that work, I owe thanks to Roger Myers, Eric Pencil and Lynn Arrington, from NASA Lewis Research Center. This thesis work owes a large debt of gratitude to Eric Pencil, whose time, patience, and advice were essential in getting the work done. His love of the Cleveland Indians is forgiven. Hani Kamhawi from Ohio State also played an invaluable role in assisting me at NASA LeRC, where his advice and assistance were invaluable. Equally as important was the assistance of WPI undergraduates Larry Byrne and Ed Cameron. Additional help was given by too many other engineers and technicians to mention, but their assistance has been greatly appreciated. Also greatly appreciated is the funding and support by the Massachusetts Space Grant Consortium and by NASA LeRC.

For three years, Professor Nikos Gatsonis has advised and supervised my work at WPI. I deeply thank him for his help, support, and advice and have learned a great deal while working in the CGPL. To my many cohorts in the lab over the last several years, including Paviii, Xuemin, Bernie, Kai, Gilmer, Tatiana, Mike and all the rest, good luck in your endeavors. You have made work enjoyable. In the department, Barbara Edilberti and Linda McClenahan provided invaluable administrative support. Thanks also to my committee members, Professors Olinger, Hermanson and Richman, and Eric Pencil. Your assistance with the final stages of this work is greatly appreciated.

There is a long list of those deserving of my personal thanks, people without whom this work would never have been completed. At the top surely must be my

parents, my brother and sister, and the rest of my family. I have too many friends at WPI to name, but every one of them has made me laugh at some point. Sanity is a wonderful thing, and you have brought it to me. To those still in Worcester, I wish you luck in your attempts to escape. To those who have left, may life treat you kindly. Finally, the greatest amount of gratitude goes to Ami, for pulling me through all of this. The future is a mystery, but happiness is not. Thank you.

Support provided by a Massachusetts Space Grant Fellowship and NASA Grant number NAG3-1873 is greatly appreciated.

Table of Contents

ABSTRACT	I
ACKNOWLEDGEMENTS	IV
TABLE OF CONTENTS	VI
TABLE OF FIGURES	VIII
NOMENCLATURE	IX
CHAPTER 1: INTRODUCTION	1
1.1 PPT FLIGHT HERITAGE, CURRENT AND FUTURE MISSIONS	5
1.2 PPT PLUMES: REVIEW OF EXPERIMENTAL INVESTIGATIONS AND MODELING	8
1.2.1 <i>Experimental Investigations</i>	8
1.2.2 <i>Computational Modeling</i>	11
1.3 OBJECTIVES AND METHODOLOGY	12
CH. 2: EXPERIMENTAL SETUP, DIAGNOSTICS AND PROCEDURES	14
2.1 EXPERIMENTAL SETUP AND FACILITY	14
2.1.1 <i>NASA LeRC Pulsed Plasma Thruster</i>	15
2.1.2 <i>Vacuum Facility</i>	16
2.1.3 <i>Probe Motion System</i>	18
2.2 PLASMA DIAGNOSTICS.....	19
2.2.1 <i>Triple Langmuir Probe Theory</i>	20
2.2.2 <i>Triple Langmuir Probe Construction and Circuitry</i>	26
2.3 EXPERIMENTAL PROCEDURES	30
2.3.1 <i>Probe Cleaning</i>	30
2.3.2 <i>Data Sampling</i>	32
CH. 3: DATA REDUCTION, ANALYSIS AND DISCUSSION OF RESULTS	35
3.1 TRIPLE LANGMUIR PROBE DATA REDUCTION AND ANALYSIS	35
3.1.1 <i>Error Analysis</i>	40
3.1.2 <i>Electron Temperature and Density of PPT Plume</i>	42
3.1.3 <i>Spatial Variation of Temperature and Density</i>	43
3.1.4 <i>PPT Discharge Energy Effects</i>	51
3.2 SINGLE LANGMUIR PROBE DATA ANALYSIS.....	52
CHAPTER 4: SUMMARY, CONCLUSIONS AND RECOMMENDATIONS	56
4.1 SUMMARY OF EXPERIMENTAL SETUP, DIAGNOSTICS AND PROCEDURES	57
4.2 SUMMARY OF DATA REDUCTION, ANALYSIS AND RESULTS	58
4.2.1 <i>Triple Langmuir Probe Data Reduction</i>	58
4.2.2 <i>Error Analysis</i>	58

4.2.3 <i>Results and Discussion</i>	59
4.3 SUMMARY OF ION VELOCITY RESULTS	60
4.4 RECOMMENDATIONS FOR FUTURE WORK	61
APPENDIX I: COMPUTER CODE	63
A.1 DATA CONVERSION BATCH FILE	64
A.2 S-PLUS SMOOTHING SCRIPT	65
A.3 TRIPLE LANGMUIR PROBE REDUCTION CODE	67
A.4 PEAK VALUE BATCH FILE	71
BIBLIOGRAPHY	74

Table of Figures

Figure 1.1: Cut away schematic of PPT, showing the plume and possible interactions with the spacecraft.....	3
Figure 2.1: Thruster schematic diagram.....	15
Figure 2.2: Probe motion system	17
Figure 2.3: Triple Langmuir probe circuit	21
Figure 2.4: Langmuir probe with sheath	22
Figure 2.5: Probe design.....	27
Figure 2.6: Electrical diagram of experimental facility	30
Figure 2.7: Glow cleaning electrode and circuit	31
Figure 2.8: Measurement locations	33
Figure 3.1: Measurement angles in parallel and perpendicular planes	36
Figure 3.2: Raw voltage and current traces with descriptions of various noises	37
Figure 3.3: Smoothed voltage and current traces for 20 J centerline measurement 14 cm from Teflon	38
Figure 3.4: Sample T_e , n_e curves for 20 J centerline, 14 cm from Teflon.....	39
Figure 3.5: Error in T_e , n_e due to smoothing	41
Figure 3.6: Comparison of smoothing and theory error.....	41
Figure 3.7: Smallest and largest peak value traces for: a)r = 6 cm, b)r=12 cm, c)r=18 cm, 10 degrees off axis in the plume of a 20J PPT	45
Figure 3.8: Electron temperature and density measurement in a PPT plume	46
Figure 3.9: Per Pulse N_e^* and T_e^* along centerline in a 20 J PPT plume.....	46
Figure 3.10: Spatial variation of N_e^* and T_e^* in a 5 J PPT plume	48
Figure 3.11: Spatial variation of N_e^* and T_e^* in a 20 J PPT plume.....	49
Figure 3.12: Spatial variation of N_e^* and T_e^* in a 40 J PPT plume.....	50
Figure 3.13: Spatial variation of N_e^* and T_e^* along centerline in 5J, 20J, and 40J PPT plume.....	51
Figure 3.14: Sample single Langmuir probe traces	52
Figure 3.15: Fast and slow ion population velocities.....	53
Figure 3.16: Sample LES 8/9 voltage discharge, [Thomasson, 1973].....	55

Nomenclature

A_n	Area of Probe n
B	Peterson/Talbot Curve Fit Parameter
C	Capacitor Capacitance
c'	Thermal Velocity
e	Charge of Electron
E	Discharge Energy
I_n	Current to Probe
I_{sp}	Specific Impulse
J_e	Electron Saturation Current Density
J_I	Ion Saturation Current Density
J_{is}	Ion Current Density at Sheath Edge
k	Boltzman constant
K_n	Knudsen Number
m_x	Mass of x
n_e	Electron Density
n_{es}	Electron Density at Sheath Edge
n_I	Ion Density
n_{is}	Ion Density at Sheath Edge
N_e^*	Average maximum electron density at a location
r_x	Axial distance from Teflon face in plane $x = \perp, $ to electrodes
r_p	Probe Radius
T^*	Time when maximum electron density is recorded
T_e	Electron Temperature
T_e^*	Average electron temperature for a location recorded at t^*
T_i	Ion Temperature
T_n	Neutral Temperature
V	Charging Voltage of Thruster Capacitor
V_{dn}	Voltage Difference between Probe n and Probe 1

V_n	Voltage of Probe n , also Velocity of Ion Population n
x	Distance
Z_I	Charge on Ion
Δt_c	Difference in Creation Time of Ion Populations
Δt_m	Difference in Measured Arrival Time of Ion Populations
α	Peterson Talbot Curve Fit Parameter
β	Constant Indicating Variation of Ion Current with Probe Potential
χ_{dn}	Non-Dimensionalized V_{dn}
χ_n	Non-Dimensionalized Probe Potential V_n
ϵ_o	Permittivity of Free Space
η	Non-Dimensionalized form of β
λ_D	Debye Length
λ_{ie}	Ion-Electron Mean Free Path
λ_{ii}	Ion-Ion Mean Free Path
θ_x	Angle from centerline in plane $x = \perp, $ to electrodes
ν_{ie}	Ion-Electron Collision Frequency
ν_{ii}	Ion-Ion Collision Frequency

Chapter 1

Introduction

In recent years, pulsed plasma thrusters, or PPTs have attracted much interest in the satellite community. The thruster's light weight, low cost, ease of operation, and reliability have all contributed to its appeal, and currently the thruster is being considered, or has been chosen, as the on-board propulsion system for several missions in the near future.

On-board propulsion includes chemical and electric thrusters, and is used for attitude control, orbit maintenance, instrument pointing and solar panel positioning, among other applications. Chemical thrusters have, until recently, been the primary on-board system, and produce thrust through the expansion in a nozzle of combustion products of a solid, liquid or gaseous propellant. Generally, chemical propulsion systems can provide large thrusts but tend to be complicated, with moving parts and volatile fuels that must be carefully stored and handled. Electric propulsion systems, such as PPTs, are fundamentally different from their chemical counterparts. In this case, thrust is generated by the acceleration of an ionized gas (plasma) through electrostatic or electromagnetic forces. Electric propulsion devices generally do not generate the large thrust common

with chemical systems, but they have far higher performance (in terms of specific impulse) and can be simpler, more reliable, and lighter than their chemical counterparts. The performance of a propulsion system is measured by its specific impulse, or I_{sp} , which is a measure of the thrust generated versus the mass expelled to generate that thrust. Chemical systems usually have I_{sp} s in the several hundreds, while PPTs as well as other electric propulsion systems have specific impulses in excess of 1000 s.

Pulsed plasma thrusters are a type of electric propulsion system that use primarily electromagnetic forces to accelerate their propellant. The thrusters have been in development since the 1950s, and have been successfully flown many times. The recent push for low power, high performance propulsion systems has brought renewed interest in PPTs, and efforts are underway to increase their performance. The current NASA goals are to reduce the flight weight by half, and to double the total impulse capability of the thruster, as compared to the LES 8/9 model PPT [McGuire and Myers, 1995].

Pulsed plasma thrusters are one of the simplest types of electric propulsion systems. Solid Teflon is used as the propellant and is spring fed to a pair of electrodes in a rail configuration. One of the electrodes also has an igniter plug, located at the face of the Teflon bar as illustrated in Fig. 1.1. In a single pulse that lasts between 5 and 20 μ s, the following events occur. First, the capacitor is charged. The spark plug then fires, emitting electrons which provide the means to initiate a discharge between the electrodes. This main discharge ablates and ionizes Teflon, and induces a magnetic field between the electrodes. The interaction between this magnetic field and the charged particles in the plasma, the $\mathbf{j} \times \mathbf{B}$ interaction known as the Lorentz force, accelerates the ionized Teflon, producing thrust. The neutrals are accelerated by gasdynamic expansion. The plasma

produced by the thruster exits the nozzle in the form of a highly concentrated blob [Cassady, 1989; Myers et al., 1995]. Because there are no pressurized liquids or gasses involved in the thruster, there is no need for valves or storage tanks. The only moving part of the propellant feed system is the spring, which pushes the fuel bar forward when the end is ablated. This, combined with the stability and durability of the Teflon propellant, makes the PPT a very safe and reliable thruster. This durability was confirmed recently when PPTs were successfully fired at NASA Lewis Research Center and Olin Aerospace after being stored in uncontrolled conditions for 20 years [McGuire and Myers, 1995].

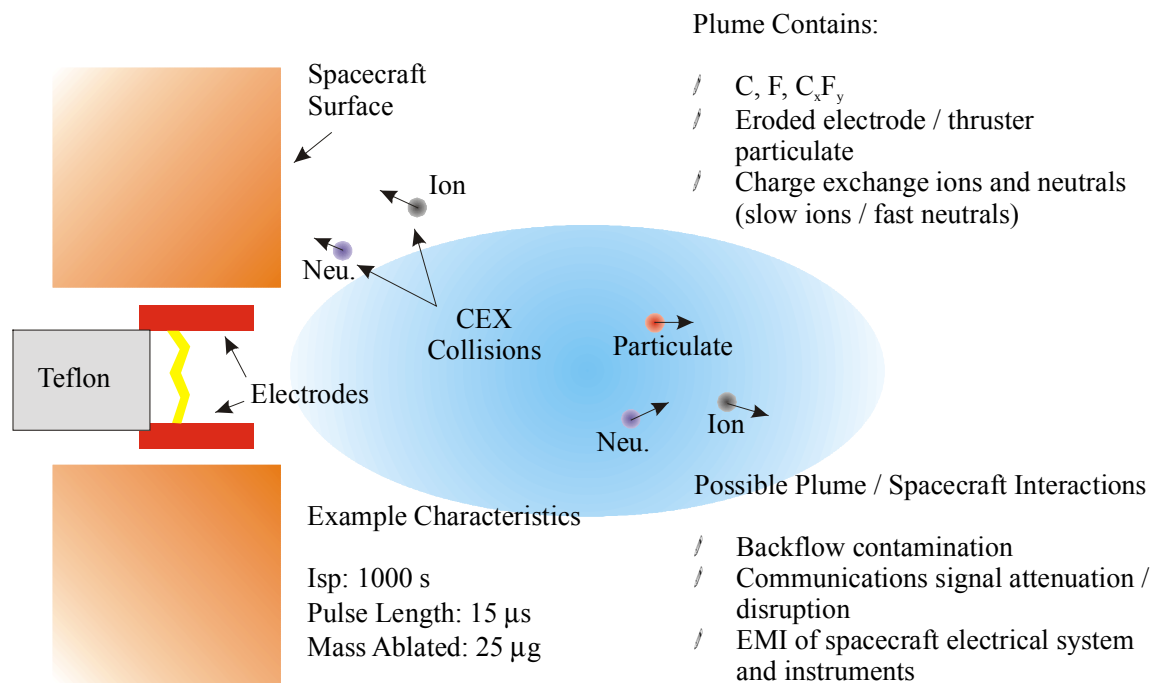


Figure 1.1: Cut away schematic of PPT, showing the plume and possible interactions with the spacecraft.

Pulsed plasma thrusters have been flown several times in the past, and are planned for several missions in the near future. Although they are low thrust devices, they are

capable of replacing current on-board systems for many applications. Proposed mission uses include: attitude control, where PPTs would replace momentum wheels, torque rods, and chemical propulsion systems; orbit maintenance, where PPTs would replace heavier and more complicated chemical propulsion systems; orbit insertion and deorbit, where PPTs would be used to raise a satellite from shuttle altitude, or deorbit a satellite at the end of its mission life. Another potential application of PPTs involves precise positioning of satellites flying in a constellation, where PPTs have the potential to be mission enabling technology [Myers et al., 1994].

Successful integration of PPTs on spacecraft requires the comprehensive evaluation of possible plume-spacecraft interactions. The PPT plume consists of neutrals and ions from the decomposition of the Teflon propellant, material from electrode erosion, as well as electromagnetic interference and optical emissions. Possible spacecraft interactions include spacecraft charging due to charged particle deposition on satellite surfaces, neutral deposition on spacecraft surfaces, erosion of satellite surfaces due to high energy plume particle collisions with spacecraft, electromagnetic interference with electronics and communications signals, and thermal loading of the spacecraft due to thruster operation.

The overall goal of the WPI PPT research program is to develop an advanced predictive ability and to assess the impact that these thrusters will have on their host spacecraft. To accomplish these goals, the WPI PPT program involves the computational modeling and experimental investigations of the PPT plume. The experiments are carried out in collaboration with NASA Lewis Research Center at the Electric Propulsion Laboratory and serve as validation for the modeling effort. Investigation of the PPT

plume properties are important in spacecraft design as well as thruster optimization and design.

This thesis details an experimental investigation of the unsteady ($\sim 20 \mu\text{s}$) plume of the pulsed plasma thruster using triple Langmuir probes to measure electron temperature and density. In addition, the analysis of ion velocity is presented based on single Langmuir probe data obtained from our previous experiments. Before the experimental work and related literature is discussed, it is important to understand the history of PPTs, and the larger context that our research exists within.

1.1 PPT Flight Heritage, Current and Future Missions

The first recorded flight of a pulsed plasma thruster occurred in 1964, when the Soviets used six PPTs on the Zond-2 satellite, to keep the satellite's solar arrays pointed to the sun. This satellite, on a Martian flyby mission, was launched on November 30, 1964 and failed to return any planetary data [Pollard et al., 1993].

Pulsed plasma thrusters were used in 1968 on the US LES-6 satellite. This thruster was designed and built by the Fairchild Hiller Corporation and MIT's Lincoln Laboratories. The LES-6 was launched on September 26, 1968 and the PPTs began operation on October 15, 1968 successfully providing east-west station keeping without interfering with telemetry or on-board communications systems [Guman and Nathanson, 1970].

MIT's development of PPTs continued for the LES 8/9 constellation of two communication satellites. The mission was designed to provide the usual uplink and downlink capabilities with the groundstation, in addition to crosslink communications between the two satellites, a technology we take for granted today [Vondra and

Thomassen, 1974]. The PPT hardware was developed for this mission to provide orbit acquisition, east-west stationkeeping, attitude control, and station changing, but was scrapped at the last minute in favor of cold gas thrusters. This flight qualified hardware has subsequently been used extensively in the experimental investigation of pulsed plasma thrusters, and has been shown to be remarkably robust. As mentioned before, these thrusters were successfully and reliably operated after 20 years on the shelf [McGuire and Myers, 1995].

The US Navy flew two PPTs on five TIP/NOVA navigation satellites in 1975, where PPTs were used on each spacecraft for drag compensation. This mission showed that PPTs had minimal contamination effects on solar arrays, and also demonstrated that with proper design, PPTs had no EMI effects on the satellite [Myers et al., 1994]. Research into PPTs continued into the late 1970s at Fairchild, where work was done on a millipound thrust level PPT [Guman and Begun, 1977]. In an experimental capacity, PPTs were flown on the Japanese ETS-IV satellite, launched in 1981, to evaluate EMI effects [Pollard, 1993].

The ETS-IV flight marked the last recorded flight of PPTs, as of 1998. Research into PPTs was revitalized in the 1990s, as NASA launched its New Millennium program, with the goal of smaller and cheaper satellites. PPTs showed great promise as an on-board propulsion system under this program and were slated for use on several missions. The EO-1 mission, for example, has a pulsed plasma thruster that will be used on an experimental basis to function as one of the satellite's momentum wheels. As of December 1998, the thruster successfully completed acceptance testing and was operated in vacuum by the spacecraft. This satellite is scheduled to be launched in 2000.

Pulsed plasma thrusters have also been proposed for use on the Deep Space 3 mission. DS-3 is a constellation of two satellites that will fly in an earth-following heliocentric orbit. They will form an interferometer with a virtual aperture, with both of the satellites collecting distant starlight, and one combining these measurements and beaming them back to earth. The very precise positioning required for this mission makes the use of PPTs very attractive, as the collector satellites will be located up to 1 km apart, within 1 cm of accuracy.

Academia, government, and industry have taken up the new research efforts into pulsed plasma thrusters. These investigations cover design, performance, and spacecraft integration with the goals of producing more efficient thrusters whose impact on their host spacecraft is well understood and minimized.

There are two basic geometric designs for the pulsed plasma thruster. The first is the rectangular design, in the style of the LES 6 and LES 8/9 thrusters. Historically, this has been the design of choice, due to its simplicity and reliability. The drawback to this design is that it develops thrust due mainly to electromagnetic forces, and any thrust due to gasdynamic expansion is not fully exploited. There are several efforts underway to develop a coaxial geometry PPT, including work at Ohio State, UIUC and the University of Tennessee [Burton, 1998]. Optimization of the rectangular geometry PPT is also being conducted at Ohio State. In their design, an inductively driven discharge circuit is used to lengthen the pulse time, providing a longer period of electromagnetic acceleration. This better utilizes the ablated fuel of the PPT, and as a side benefit eliminates the severe discharge voltage reversal on the capacitor, thus lengthening its life [Turchi, 1997].

An addition to the Teflon PPT variant of the PPT design involves the use of a gas propellant instead of solid Teflon. Among other benefits, this serves to increase the utilization efficiency of the thruster. The main drawback of the gas fed pulsed plasma thruster is the increased complexity due to the gas propellant system and its associated plumbing. Research into the GFPPT is currently being carried out at Princeton and at NASA's Jet Propulsion Laboratory [Ziemer, et al., 1997].

1.2 PPT Plumes: Review of Experimental Investigations and Modeling

The plume of the PPT consists of a series of plasma blobs ejected during thruster firing. The plume contains neutral and charged particles from the decomposed Teflon propellant bar and eroded particulate from the thruster electrodes and nozzle parts, as shown in Fig. 1.1. Ions or neutral plume particles from the plume may deposit on the spacecraft and contaminate sensitive instruments or solar arrays. There is also concern that the plume may cause communication signal attenuation and electromagnetic interference with the spacecraft electrical bus. Knowledge of plume composition is essential in determining possible spacecraft interactions. In addition, plume composition can reveal important information with regard to the PPT operation and its acceleration mechanisms. As such, plume studies were initiated early in the PPT development cycle.

1.2.1 Experimental Investigations

The LES-6 thruster plume was the first to be extensively investigated. This thruster operated at 1.85 J and ablates 10 μg of propellant during a 3 μs discharge to produce a specific impulse of 312 s. Vondra et al. [1970] found, using thrust stand and

Faraday cup measurements, that ion velocities were on the order of 40,000 m/s. They were also able to deduce that neutral velocities were approximately 3,000 m/s. A microwave interferometer was used to infer maximum plasma density equal to $3 \times 10^{18} \text{ m}^{-3}$ at 20 cm downstream of the Teflon face. Using single Langmuir probes, they measured electron temperatures on the order of 20 eV [Vondra et al., 1970]. These temperatures are approximately an order of magnitude high, compared to other investigations, and these erroneous results illustrate the difficulty in using Langmuir probes in the unsteady, noisy plume of the PPT. A subsequent study of the LES 6 plume used spectroscopy to measure velocities of specific components in the PPT plume [Thomassen and Vondra, 1972]. This work identified excited neutral, singly, doubly and triply ionized carbon and fluorine. Measured velocities ranged between 4000 m/s for neutral fluorine to 35,000 m/s for triply ionized carbon. They also used a Faraday cup to estimate that the plume is 10% ionized, confirming the presence of a significant neutral efflux.

Mass spectrometers were used to study the composition of the plume of the Japanese ETS-IV pulsed plasma thruster [Hirata and Murakami, 1984]. This study identified various amounts of C, CF, CF₂ and CF₃, in the plume. Deposition measurements identified the plume divergence to be approximately 40 degrees, defined by measuring the angle where the contamination thickness was half that at the center of the target.

Several plume studies on millipound thrust level PPTs were completed in the 1970s. The Fairchild Republic Co. studied this class of PPT, using double Langmuir probes. Guman and Begun [1978] found that at 0.7 m from the thruster along the

centerline, peak ion densities were on the order of 10^{19} m^{-3} and that electron temperatures were around 2 eV.

Laser interferometers and Langmuir probes were also used to measure density in the plume of a high energy (80 - 100 J) Russian PPT, finding maximum plasma densities to be approximately 10^{21} m^{-3} at a location 13 cm from the Teflon surface [Antropov et al., 1997]. Triple Langmuir probes were recently used to study the plume of a coaxial PPT, finding densities on the order of 10^{22} m^{-3} and temperatures around 0.75 eV at a location 1 cm from the exit plane of the nozzle [Bushman et al., 1998].

Because of the availability of LES 8/9 flight hardware, its plume has been studied extensively. Initial studies included contamination assessments using quartz slides, planar Langmuir probes for measurements of ion current density and single Langmuir probes for determination of ion velocity [Carter and Heminger, 1995; Myers et al., 1996]. The study found that measurable changes in transmittance of the quartz slides were confined to 30 degrees, centerline ion velocity of approximately 40 km/s and an ion density of $6 \times 10^{18} \text{ m}^{-3}$ at a distance of 24 cm from the thruster. Subsequent investigations by Eckman et al. [1998] using single Langmuir probes mapped ion velocity and found two waves of ions in the plume of the LES 8/9, travelling at velocities of approximately 30 and 60 km/s respectively. In the same study, the composition of the PPT plume was qualitatively studied using a residual gas analyzer, identifying C, F, C_xF_y , and various thruster materials, results similar to those of Hirata and Murikami [1984]. Additionally, fast ionization gauges were used and detected the presence of slow neutral particles up to 1 ms after the discharge had ended, indicating an inefficient use of the propellant [Eckman et al., 1998].

Research at the Air Force Research Laboratory at Edwards Air Force Base has included studies of inefficiencies in the propellant utilization of the PPT, and have identified large particulate emission in the PPT discharge, accounting for approximately 20% of the ablated mass while producing negligible thrust [Spanjers et al., 1998]. ARFL researchers have also studied methods of reducing propellant consumption while preserving thrust levels, improving the performance of the PPT by 25% [Spanjers et al., 1997].

1.2.2 Computational Modeling

The development of a computational model of the PPT plume is very important in the effort to determine possible plume/spacecraft interactions. As described earlier, the plume of the PPT consists of a relatively dense mixture of ions, electrons, and neutral particles, providing an ample challenge to the computational modeler. Because of the nature of the plume, interactions between all these species must be correctly considered in order to properly assess contamination and backflow from the PPT.

The model under development at WPI combines Direct Simulation Monte Carlo, Particle In Cell, and fluid methodologies to account for the charged and neutral components in the plume [Gatsonis and Yin, 1997a; 1997b]. In DSMC, the flow is treated as a collection of kinetic macroparticles, with each particle representing a large number of molecules in the actual flow. Modeling the PPT plasma flow requires the simulation of charged particle interactions, and the model under development uses a modified PIC methodology to account for ion-neutral interactions. Finally, the model accounts for electrons as well as ion-electron collisions using fluid methodologies [Gatsonis and Yin, 1998].

Important in any computational simulation are the initial and boundary conditions imposed, as well as proper code validation. Of particular importance is the particle injection at the exit plane of the thruster. Experimental investigation of the PPT plume provides model inputs at the thruster exit plane and validation of plume behavior downstream of the thruster exit [Yin et al., 1999 (in preparation)].

1.3 Objectives and Methodology

The primary goal of this investigation is to measure electron temperature and density in the plume of a LeRC PPT operating at energy levels between 5 and 40 J. This energy range corresponds with proposed missions in the near future. This experimental investigation is part of an effort to characterize the PPT plume in order to assist in the evaluation of potential plume-spacecraft interactions and to develop the ability to predict their impact.

Diagnostics used for electron density and temperature measurements in plasmas include single and double Langmuir probes, spectroscopic and Interferometric methods. Single and double probes have the disadvantage of requiring relatively long or reliably repeatable measurements to obtain one data point, while optical and Interferometric methods are hampered by the complexity of the required apparatus. In the very short duration (approximately 15 μ s) pulse discharge of the PPT, the triple probe shows great opportunity to easily and reliably measure electron temperature and density. The challenges of using the probes in the PPT plume include the electrically noisy nature of the discharge and the short duration of the pulse, which requires very accurate and sensitive measuring devices.

The goals of this thesis are:

- Design a setup that implements the use of triple Langmuir probes in the plume of the LeRC-PPT using the facilities at NASA Lewis Research Center. This task includes the following subtasks:
 - Review previous triple probe work and determine their applicability to PPT plumes.
 - Design and build a working triple Langmuir probe setup.
 - Establish procedures for testing and related tasks, such as probe cleaning.
- Design and build a moveable stand to allow accurate positioning of probes from outside the vacuum facility. This will greatly increase the amount of data that can be collected in a short amount of time, due to the relatively long pump down time of the facility.
- Use the triple Langmuir probes to take electron temperature and density measurements in the plume of a LeRC-PPT in the planes perpendicular and parallel to the thruster electrodes. Data was collected at centerline, and at 10, 20, 30 and 45 degrees off of centerline at thruster energy levels of 5, 20 and 40 J, corresponding to the range of energies for currently proposed missions using available technology.
- Establish data reduction procedures and develop computer codes to implement triple Langmuir probe theory.
- Perform error analysis, analyze results, and examine the spatial and temporal variation of plume properties, as well as effects of thruster energy level.

Chapter 2

Experimental Setup, Diagnostics and Procedures

One of the goals of this work is to apply plasma diagnostics in the unsteady plume of the PPT to obtain electron temperature and density. Indeed, among the accomplishments of this work is that these measurements were successfully taken and so it is especially important to describe in detail the experimental setup, diagnostics and procedures that were developed. The theory behind the triple Langmuir probe diagnostics will be discussed, as will the construction and use of the probes. The experimental procedures will be outlined to assist future investigators in this area.

2.1 Experimental Setup and Facility

All experiments were carried out at NASA Lewis Research Center Electric Propulsion Laboratory. To simulate the space environment that PPTs operate in, all experiments were carried out under a vacuum using the bell jar VACFAC 54. Because it is laborious and time consuming to manually reposition the probes between each measurement, a probe translation system was built that allows the probes to be moved outside of the bell jar. The construction, circuitry and electronics related to triple

Langmuir probe measurements will be described as well as the procedures used for glow cleaning the probes.

2.1.1 NASA LeRC Pulsed Plasma Thruster

All temperature and density measurements in this thesis were taken in the plume of the LeRC laboratory model PPT. This thruster was built for both component life tests and plume characterization studies, and is illustrated in Fig. 2.1. The thruster has a parallel electrode configuration, in the heritage of the LES 6 and LES 8/9 designs. The electrodes are 2.5 cm long with a 3.8 cm gap. A spark plug is located at the base of the cathode, to initiate the discharge when the thruster fires. A solid bar of Teflon 2.5 x 3.8 cm square is spring fed to the electrodes and held in place by a 1.5 mm notch in the anode. The electrodes are surrounded by a Torlon 5530 casing that is 6.4 cm wide across the electrodes and 4.4 cm along the electrodes. A 33.3 μF capacitor capable of storing approximately 60 J is used to store the energy just prior to discharge.

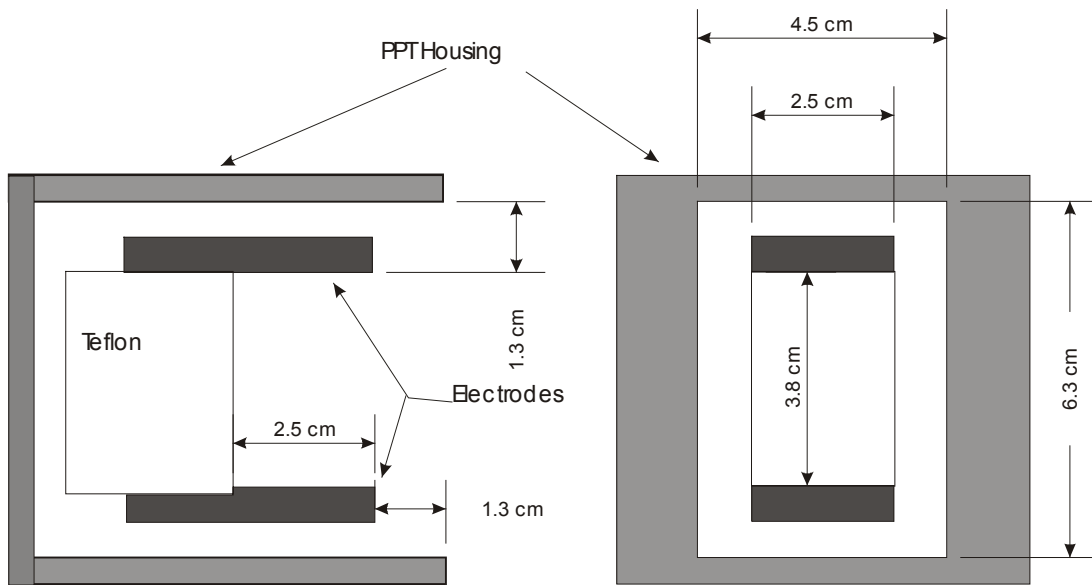


Figure 2.1: Thruster schematic diagram

Preliminary performance measurements were made on a thrust stand for the LeRC PPT. The thrust stand works by measuring the displacement that the thruster causes on a moment arm when it is fired. From calibration, this displacement is related to an impulse bit $I_{bit} = \int_0^P T dt$, the thrust integrated over the pulse period $P=15\mu s$. I_{bit} is measured in two ways for the PPT, in single pulse mode, and in continuous firing mode, and for the lab model PPT used in this study, these two modes agree to within 2%. To measure mass ablated per pulse, the thruster is fired for an hour at a known rate. The fuel bar is weighed before and after the test, and from this data the average mass loss per pulse can be calculated. Specific impulse can be found by dividing the impulse bit by the mass loss per pulse and the acceleration of gravity [Pencil, 1998]. Performance parameters are presented in Table 2.1 for energy levels used in the experimental measurements. Uncertainty in mass loss data for the 5 J case prevents the calculation of I_{sp} .

Discharge Energy (J)	Impulse Bit ($\mu N\cdot s$)	Mass Loss/Pulse ($\mu g/pulse$)	Specific Impulse (s)
5.3	36	-	-
20.5	256	26.6	982
44.0	684	51.3	1360

Table 2.1: Performance Characteristics of LeRC PPT.

2.1.2 Vacuum Facility

All triple Langmuir probe measurements were taken in VF 54, a bell jar located in the Electric Propulsion Laboratory at NASA LeRC. This bell jar is 1 meter tall, with a diameter of 0.5 m. It has a mechanical roughing pump, and an oil diffusion pump that held a vacuum of 1.5×10^{-5} Torr with an approximate pumping time of 5 hours. At room

temperature, this pressure results in a number density of about $4 \times 10^{17} \text{ m}^{-3}$ and an ambient mean free path of over 2.5 m.

The probe motion assembly with the attached thruster was placed at the bottom of the bell jar, and the thruster was oriented so that it always fired upward, along the long axis of the facility as shown in Fig. 2.2. One concern in taking plasma measurements in a facility as small as this one is that the plasma will reflect off of the far wall back to the probe before a complete measurement could be taken. Assuming that the fastest part of the plasma travels at 60 km/s [Eckman et al., 1998], for probes that are located 20 cm from the thruster, and a thruster exit 90 cm from the top wall of the tank, the plasma will reflect to the probe in 2.66 ms, much longer than the PPT pulse.

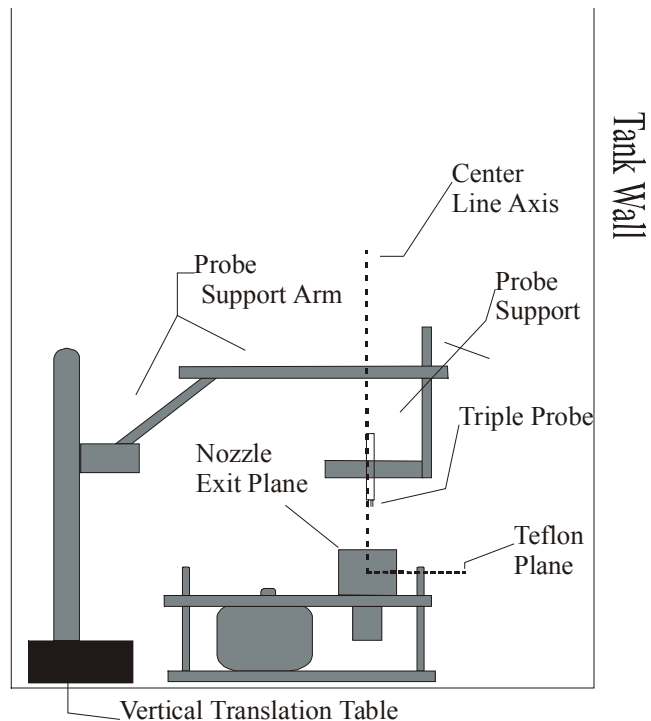


Figure 2.2: Probe motion system

2.1.3 Probe Motion System

Because of the length of time required to pump down the bell jar, it was desirable to design a system that would allow for reposition of the Langmuir probes during testing. To achieve this goal, a stepper motor driven translation table was used to move the probes axially in the plume, to allow a range of measurements at a set angle off of thruster centerline. A schematic of this arrangement is shown in Fig. 2.2. The translation table is mounted vertically in the tank, on a flat base. The thruster is mounted on this base, via 1/8" threaded rods which are flexible, and allow the thruster to be positioned so that measurements may be taken at up to 45 degrees off the centerline. A pivoting arm is attached to the translating stage, and on the end of this is attached a 1/4" threaded rod, which hangs from the arm. The probes are attached to the end of this rod by sandwiching them between two thin sheets of metal, which are screwed together to tightly hold the probes in place.

This apparatus is able to reposition the probes from the exit plane of the thruster to 20 cm from the face of the Teflon, and the pivoting arm allows the probes to be manually centered above the thruster as it is rotated through various positions. Motion of the stage is controlled by a computer program, which takes as input the desired distance to move the probe and returns the new location in centimeters from the Teflon face. The use of the probe motion system greatly increased the amount of data that could be collected in the short facility time available for this project.

2.2 Plasma Diagnostics

Electrostatic, or Langmuir probes were the first diagnostics developed capable of taking measurements inside of a plasma. Physically they are very simple consisting only of an exposed wire in a plasma that is biased to some potential. One of the drawbacks of most Langmuir probes is that a voltage vs. current curve is needed to properly determine plasma properties from the probe measurements. This V-I curve is developed by sweeping the voltage applied to the probes and measuring the current collected, and is used to determine temperatures and densities in the plasma, through appropriate formulae [Chen, F. F., 1965].

The symmetric triple Langmuir probe solves the problem of this voltage sweep allowing for the instantaneous measurement of electron temperature (T_e) and density (n_e), where previously, tedious curve fitting was required. The symmetric triple probe consists of three exposed wires of equal area in the plasma. By correctly biasing the probes, and using the theory outlined in the following chapter, electron temperature and density can be found.

Triple Langmuir probes have been used extensively for diagnostics in the plumes of electric propulsion devices. The first application was by Myers [1989] on MPD thruster plumes. A subsequent study found electron densities of 10^{19} m^{-3} and electron temperatures of $\sim 2 \text{ eV}$, data similar to that expected in the PPT plume. This work considered many experimental concerns with the probes, including probe misalignment, contamination effects and the variation in ion sheath size, and has been widely cited by subsequent triple probe work in EP plumes [Tilley, 1990]. Research has extended the capability of the triple probe to include the measurement of ion temperature as well. This

so-called quadruple probe operates on similar principles as the triple probe, and has been used in the plasma exhaust of arcjets and a coaxial pulsed plasma thruster. In both cases, measured values are on approximately the same order as those expected in the PPT plume [Bufton et al., 1995; Bushman et al., 1998]. Triple probes have also been used at MIT in the plume of the SPT-70 Hall Thruster [Fife and Martinez-Sanchez, 1998] and to measure high enthalpy air plasma flow properties at Stuttgart University [Habiger and Auweter-Kurtz, 1996].

Efforts to apply triple Langmuir probes in the PPT plume have been underway for several years but was plagued by problems with grounding and electronics [Eckman and Santesson, 1996; Papini and Slade, 1997]. This study details the successful completion of this work, including the theory, equipment, and data reduction required to arrive at the results.

2.2.1 Triple Langmuir Probe Theory

As the name suggests, a triple probe consists of three exposed wires. A fixed voltage is applied between two of those wires, generating a current in that circuit, which is measured. The voltage difference between the positive wire and the third wire, which is electrically floating, is also measured, as shown in Fig. 2.3. Using the methods described below, these two values allow for the evaluation of the electron temperature, and subsequently the electron density.

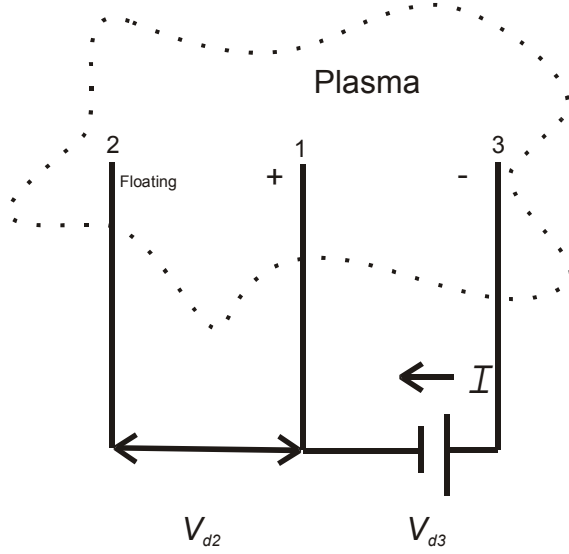


Figure 2.3: Triple Langmuir probe circuit

Triple Langmuir Probe theory and design was first derived and implemented by Chen and Sekiguchi [1965]. A sheath forms around any biased surface in a plasma, due to the attraction of one charged species, and the repulsion of the opposite charge, and is illustrated in Fig. 2.4. In the thin sheath approximation, it is assumed that the sheath thickness λ_s is much smaller than the probe radius $\lambda_s \ll r_p$, and so the measuring area of the probe can be considered to be the surface area of the exposed wire. Because all the wires have the same radius, the assumption that all probes collect over the same area can be made. An equation describing the current to each electrode, shown in Fig. 2.4, can be written for probes -1, -2 and -3 respectively as follows:

$$I_1 = A_1 [J_e \exp(-\chi_1) - J_i(\chi_1)] \quad [2.1]$$

$$I_2 = A_2 [J_e \exp(-\chi_2) - J_i(\chi_2)] \quad [2.2]$$

$$I_3 = A_3 [J_e \exp(-\chi_3) - J_i(\chi_3)] \quad [2.3]$$

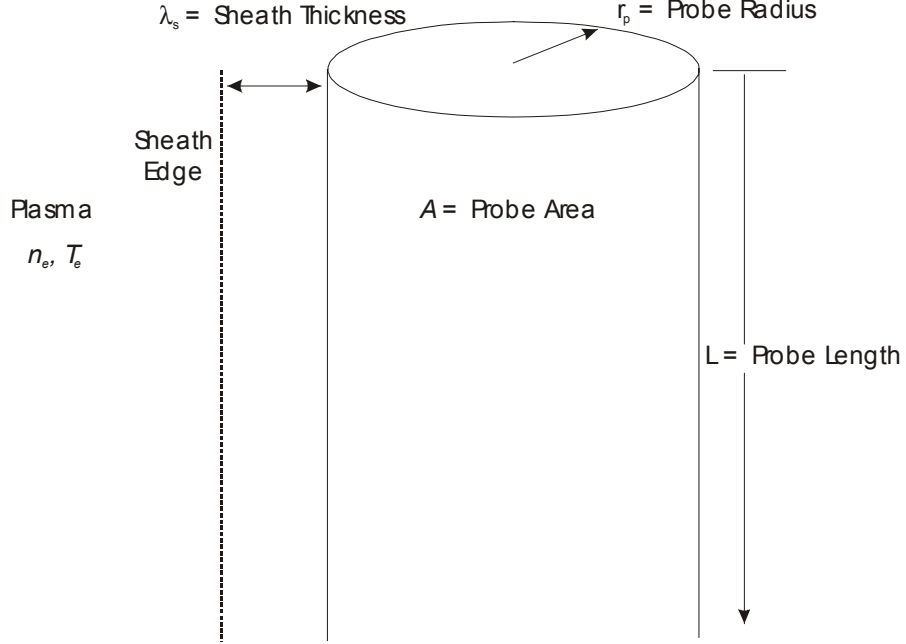


Figure 2.4: Langmuir probe with sheath

In the above expressions, $J_e = n_e e (kT_e / 2\pi m_e)^{\frac{1}{2}}$ is the electron current density due to the thermal diffusion of electrons to the sheath edge; J_i is the ion saturation current density; $\chi_n = e|V_n - V_p| / kT_e$ is the non-dimensional potential of the electrode V_n with respect to the plasma potential V_p ; e is the charge of a single electron, and k is the Boltzman constant. The area of each probe is designated by A_1 , A_2 , and A_3 respectively and are assumed to be equal.

The variation of the ion saturation current due to a change in probe potential is assumed to be negligible when compared to the variation in electron current, so it is assumed that $J_1 = J_2 = J_3$. Since probe -2 is floating, $I_2 = 0$, and thus $I_1 = I_3 = I$ as a result of Kirchoff's law. If the Eqs. 2.1 and 2.2 are added and then divided by the sum of Eqs. 2.1 and 2.3, the resulting equation is:

$$\frac{1}{2} = \frac{1 - \exp(-\chi_{d2})}{1 - \exp(-\chi_{d3})} \quad [2.4]$$

with $\chi_{dn} = \chi_n - \chi_1 = \frac{e|V_n - V_p| - e|V_1 - V_p|}{kT_e}$ for $n=2,3$. As is evident, the plasma potential

V_p cancels from Eq. 2.4, which can be rewritten as:

$$\frac{1}{2} = \frac{1 - \exp\left(-\frac{eV_{d2}}{kT_e}\right)}{1 - \exp\left(-\frac{eV_{d3}}{kT_e}\right)} \quad [2.5]$$

V_{d3} is a constant input to the probe and V_{d2} is measured output, therefore Eq. 2.5 can be solved to provide T_e .

Triple Langmuir probes provide T_e and J_i , and to obtain the electron density directly from the output, the model of Chen and Sekiguchi [1965] needs to be utilized. The ion current density at the plasma sheath edge of the probes can be approximated if $T_e \gg T_i$ using the equation:

$$J_i = en_{is} \left(\frac{kT_e}{m_i} \right)^{\frac{1}{2}} \quad [2.6]$$

with n_{is} the density at the sheath edge, and m_i the mass of the ion species. In plasmas where $T_e \cong T_i$, this equation will only be off by, at most, a factor of about $\sqrt{2}$. By making the assumptions that the plasma is quasineutral at the sheath edge, i.e. $n_{is} = n_{es}$, that the electrons have a Maxwellian energy distribution and that the Bohm sheath criteria holds, the following equation can be written:

$$n_{is} \cong n_{es} = n_e \exp\left[-\frac{e}{kT_e} \left(\frac{kT_e}{2e} \right)\right] = n_e \exp\left(-\frac{1}{2}\right) \quad [2.7]$$

If the sheath area is approximately equal to the probe area, then using Eqs. 2.6 and 2.7

$$J_{is} = J_i = \exp\left(-\frac{1}{2}\right)en_e\left(\frac{kT_e}{m_i}\right)^{\frac{1}{2}} \quad [2.8]$$

Through some manipulation of Eqs. 2.2 and 2.3, and using the assumptions used to arrive at Eq. 2.5, the ion current density J_i can be written as

$$J_i = (I / A)(\exp(\chi_{d2}) - 1) \quad [2.9]$$

Equating this expression with the ion current density Eq. 2.8, the electron density can be solved for as a function of current measured in the probe I , and electron temperature obtained through Eq. 2.5, as shown

$$n_e = \left(\frac{\sqrt{m_i}}{A} I\right) \frac{\exp(1/2)}{e\sqrt{kT_e}[\exp(\chi_{d2}) - 1]} \quad [2.10]$$

Equations 2.5 and 2.10 now can be used to find the electron temperature and density in the so called “thin sheath approximation”. Chen [1971] introduced corrections for this assumption in an attempt to provide a more correct solution of T_e and n_e . This correction stems from the fact that the electrodes are biased to different potentials, and thus will have different sheath areas. The application of this theory by Tilley et al. [1990] will be used in the following discussion and analysis, since it is directly applicable to the plasma being studied here.

The ion flux to a probe aligned with the plasma flow vector can be written as a function of the nondimensional probe potential, χ , using the Peterson/Talbot curve fit of James Laframboise’s calculations. This curve fit is given as

$$J_i(\chi) = J_{io}(B + \alpha)^\alpha \quad [2.11]$$

where the ion current at the sheath edge is

$$J_{io} = n_i Z_i e_i \left(\frac{Z_i k T_e}{2 \pi m_i} \right)^{1/2} \quad [2.12]$$

and Z_i is the charge number of the ions. The curve fit parameters in Eq. 2.11 are given by

$$\alpha = 2.9 / \left[\ln(r_p / \lambda_D) + 2.3 \right] + 0.07 (T_i / Z_i T_e)^{0.75} - 0.34 \quad [2.13]$$

$$B = 1.5 + \left(0.85 + 0.135 \left[\ln(r_p / \lambda_D) \right]^3 \right) (T_i / Z_i T_e) \quad [2.14]$$

where the Debye length $\lambda_D = \sqrt{\epsilon_o T_e / e n_e}$. Chen and Sekiguchi [1965] noted that "...the square of the ion current... varies almost linearly with the difference between the actual probe potential and the floating potential." This leads to

$$J_i^2(V) = J_i^2(V_f) \left[1 + \beta(V - V_f) \right] \quad [2.15]$$

where β is a constant that indicates the variation of ion current as a function of probe potential. This constant can be written as the non-dimensional parameter η through the relation

$$\eta = \beta \left(\frac{k T_e}{e} \right) \quad [2.16]$$

and η can also be found using a non-dimensional form of Eqs. 2.15 and 2.11 such that

$$\eta = \frac{2\alpha}{B + \chi_f} \quad [2.17]$$

If the electron and ion currents are equated in Eq. 2.2, the non-dimensional floating potential χ_f can be found using the relation

$$\left[B + \chi_f \right]^{2\alpha} - \frac{M_i}{m_e} \exp(-2\chi_f) = 0 \quad [2.18]$$

Improved equations for electron temperature and density can now be written as follows:

$$\frac{1}{2} = \frac{1 - \frac{1}{2} \left([1 - \beta V_{d2}]^{1/2} + [1 + \beta(V_{d3} - V_{d2})]^{1/2} \right) \exp(-\chi_{d2})}{1 - \exp(-\chi_{d3})} \quad [2.19]$$

$$n_e = \frac{\exp\left(\frac{1}{2}\right) \frac{I}{A_3} \left(1 - \eta \left(\chi_f - \frac{1}{2}\right)\right)^{1/2}}{e \left(\frac{kT_e}{M_i}\right)^{1/2} \left([1 + \eta(\chi_{d3} - \chi_{d2})]^{1/2} - \exp(-(\chi_{d3} - \chi_{d2}))\right)} \quad [2.20]$$

It is evident from the above expressions that as β approaches zero, Eq. 2.19 takes the form of the thin sheath approximation of T_e and Eq. 2.20 reduces to Eq. 2.10, the thin-sheath density equation.

2.2.2 Triple Langmuir Probe Construction and Circuitry

Proper construction of the triple Langmuir probes and especially their circuitry is very important to their successful use. The triple probe consists of three exposed wires aligned with the plasma flow. These wires were 0.25 mm diameter tungsten fed through four bore alumina tubing with a diameter of 6.28 mm, with 9 mm of wire exposed at the tip of the probe. The alumina tubing serves to insulate the wires from the probe support and also holds the wires at a fixed separation, keeping them aligned with the flow. This design is illustrated in Fig. 2.5.

It is important to verify that the probe dimensions chosen are proper, in that the theory presented in the previous section is applicable for plasma values expected in the PPT plume. Application of triple probes requires that several conditions be met. These conditions stem from the approximations made in the derivation of the probe theory. The charged particles in the plume must exhibit free molecular flow on the length scale of the probe radius, thus the Knudsen number $Kn = \lambda/r_p$ must be much greater than 1 for both

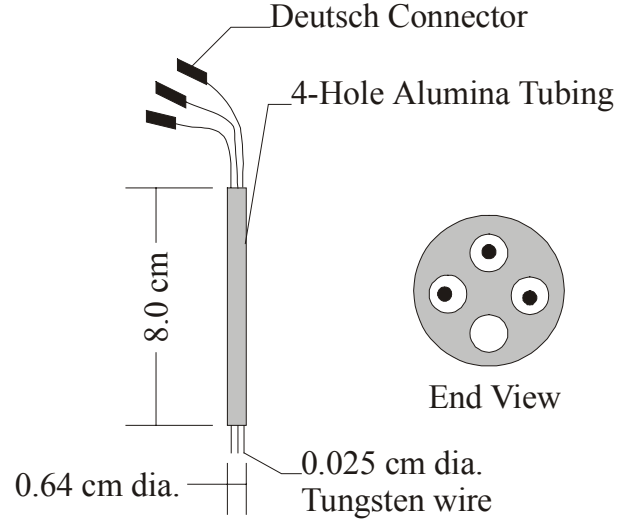


Figure 2.5: Probe design

ion-ion and ion-electron collisions. To ensure that the thin sheath approximation holds, the mean free path for ion-ion, λ_{ii} , and ion-electron, λ_{ie} , collisions must be much greater than the Debye length and the requirement for the Peterson/Talbot curve fit is that the probe radius is between 5 and 100 times the Debye length. The mean free paths are given by:

$$\lambda_{ii} = \frac{c'_i}{v_{ii}} \quad [2.21]$$

$$\lambda_{ie} = \frac{c'_e}{v_{ii} \sqrt{\frac{m_i}{2m_e} \left(\frac{T_i}{T_e} \right)^{\frac{3}{2}}}} \quad [2.22]$$

where the mean thermal speed for the species $P=i,e$ is

$$c_P' = \sqrt{\frac{8kT_P}{\pi m_P}} \quad [2.23]$$

and the ion collision frequency is

$$v_{ii} = n_i c_{ii}' 6\pi b^2 \ln\left(\frac{\lambda_D}{b}\right) \quad [2.24]$$

In the above expression, b is the impact parameter given as

$$b = \frac{e^2}{4\pi\epsilon_0 m_i c_{ii}'^2} \quad [2.25]$$

Estimates of minimum and maximum number density and conditions of applicability of triple probes in the PPT plume are obtained assuming:

$n_e = n_i =$ a) $1 \times 10^{18} \text{ m}^{-3}$, b) $1 \times 10^{20} \text{ m}^{-3}$, $T_i = T_n = 0.5 \text{ eV}$ and $T_e = 3 \text{ eV}$.

Parameter	Collision Type		Required Value
	i-i	i-e	
$Kn = \frac{\lambda}{r_p}$	a) 81	22821	$\gg 1$ (free molecular flow)
	b) 1.1	303	
$\frac{\lambda}{\lambda_D}$	a) 794	225101	$\gg 1$ (thin sheath)
	b) 105	30000	
$\frac{r_p}{\lambda_D}$	a)	9.86	$5 \leq \frac{r_p}{\lambda_D} \leq 100$
	b)	97	

(Peterson / Talbot curve fit)

Table 2.2: Triple Langmuir probe criteria and calculated values for PPT plume

These calculations ensure that the probes meet all conditions, with the exception that the ion-ion Knudsen number (λ_{ii}/r_p) is not much greater than unity as the densities reach $1 \times 10^{20} \text{ m}^{-3}$. The error that this introduces into the measurements will be discussed in the appropriate section, but does not greatly impact the measurements. If T_i is larger than predicted above, the results improve and the ion-ion Knudsen number condition is met. For example, with $T_i = 2 \text{ eV}$, $Kn_{ii} = 14.28$.

After the probe wires pass through the alumina tubing they were connected to deutch pins, and insulated with heat shrink tubing. Each of these pins was connected to

the center conductor of a BNC coaxial cable. The insulator shields of these cables was isolated at the probe tip end, and the cables were run along the probe arm and down to an isolated BNC feed through to pass the signal outside of the vacuum facility. On the outside of the facility the shielding of the probe data cables was grounded to a common ground plane.

This ground plane served as a common ground for the thruster, probe shielding, and Faraday cage that protected the electronics. All metal thruster and probe support surfaces were electrically insulated from the vacuum chamber walls, so that a single, common ground was used for the entire setup. During initial testing a lot of effort was devoted to eliminating noise from the probe output, and this grounding configuration seemed to provide the most reliable probe operation.

From the outside of the bell jar, the three probe signal wires were connected to the triple probe circuitry. This circuitry is based on the design outlined in Tilley et al. [1990], and is illustrated in Fig. 2.3. An electrical diagram of the entire vacuum chamber, including the thruster and probe electronics is shown in Fig. 2.6. In this circuit, V_{d3} is fixed and provided by three 9-Volt batteries. This voltage was measured before each set of data was collected, ranged between 24 and 28 volts and was found to vary by not more than 0.01 V during a single set of measurements. The voltage difference V_{d2} was measured by recording V_1 and V_2 on an oscilloscope using 10:1 voltage probes, and then subtracting these signals digitally on the oscilloscope. The current I_3 was measured using a Tektronix model TM503 Hall effect current probe. All data was recorded on a Lecroy model 9314M oscilloscope, and saved to floppy disk for later reduction.

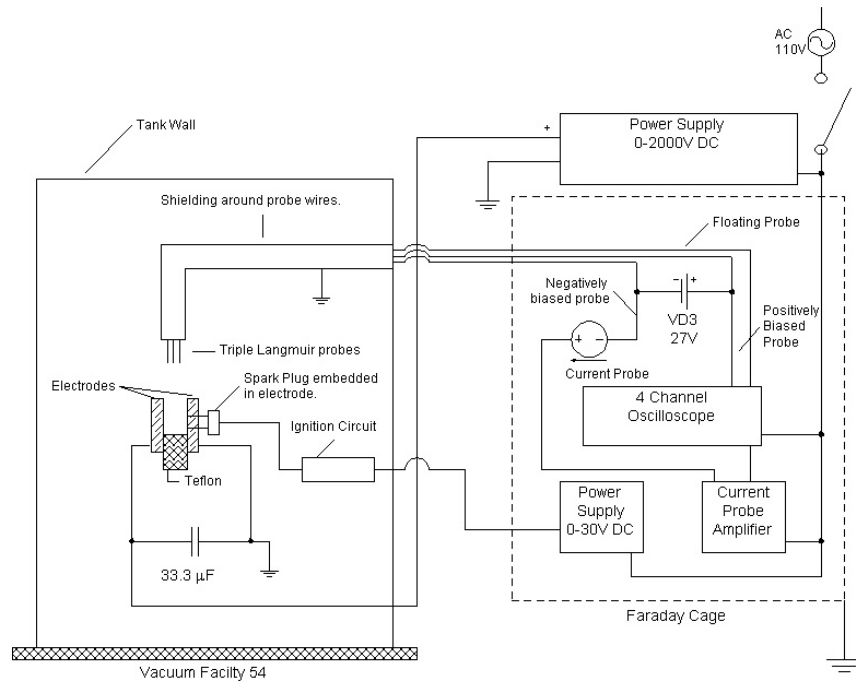


Figure 2.6: Electrical diagram of experimental facility

2.3 Experimental Procedures

2.3.1 Probe Cleaning

An important consideration when using Langmuir probes is the elimination of possible contamination effects. In the case of PPTs, it was noticed that after firing for multiple pulses, a black residue was deposited on the probe tips and alumina tubing. Because of concerns that this contamination might affect the measurements, a glow cleaning apparatus and procedure was devised.

During glow cleaning, an arc is struck between the probe tip and an electrode, and this arc cleans the probe of any contaminants. Glow cleaning requires an electrode adjacent to the probe tips, and in previous triple Langmuir probe applications,

investigators have used a thruster electrode for this purpose [Tilley et al., 1990]. There was concern that using the PPT anode would damage the PPT's electronics, so an electrode was mounted on the probe-support arm, about 2 cm from the probe tips. This electrode was insulated from the probe-support arm and was connected to an isolated feed through, which could be connected to a high-voltage supply on the instrument rack. A diagram of the glow cleaning circuit is shown in Fig. 2.7. To strike an arc between the cleaning electrode and the probe tip, the pressure in this small area must be raised. To accomplish this, an argon gas-feed system was constructed using a flexible length of Tygon tubing to deliver the gas from a feed through to the probe tip area. A Nupro regulator valve and a needle bleed valve were used to control gas flow between the argon bottle and the feed through.

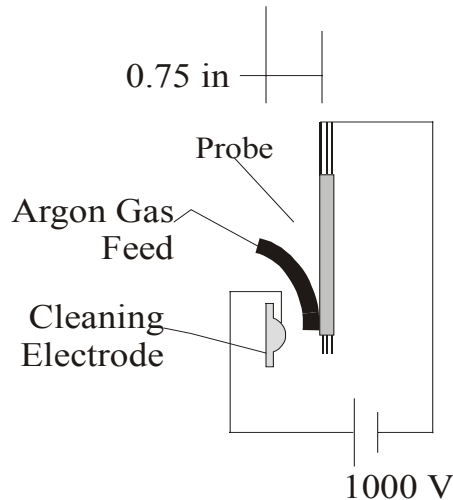


Figure 2.7: Glow cleaning electrode and circuit

During the cleaning procedure, the probes were first disconnected from the electronics, and connected to the ground on the high voltage supply. The thruster was also disconnected from the high voltage supply, and the capacitor was fully discharged. The cleaning electrode was then connected to the high voltage supply, and the voltage was set to about 1000 V. The gate valve separating the oil diffusion pump from the bell jar was closed, and argon gas was bled into the bell jar, with the flow rate controlled by the needle valve. The introduction of argon to the area of the probe tip eventually allowed a current to flow between the electrode and the probe wires. This discharge lasted for about 8-10 seconds, at which time the pressure in the facility rose to the point where the arc attached to other metal surfaces. At this time, both the gas feed and the power supply to the electrode were turned off. It was established that the 8 to 10 second period of discharge was sufficient to clean the probe tips of most of the deposited contaminants.

2.3.2 Data Sampling

Triple probe measurements were obtained on planes parallel and perpendicular to the thruster electrodes. The set of measurement locations is shown in Fig. 2.8. Centerline measurements were collected first, followed by measurements in the plane perpendicular to the electrodes at 10, 20, 30 and 45 degrees off the thruster centerline. These measurements were repeated for 10, 20 and 30 degrees off centerline in the plane parallel to the thruster electrodes. Measurements in the perpendicular plane were taken on the anode side of the thruster.

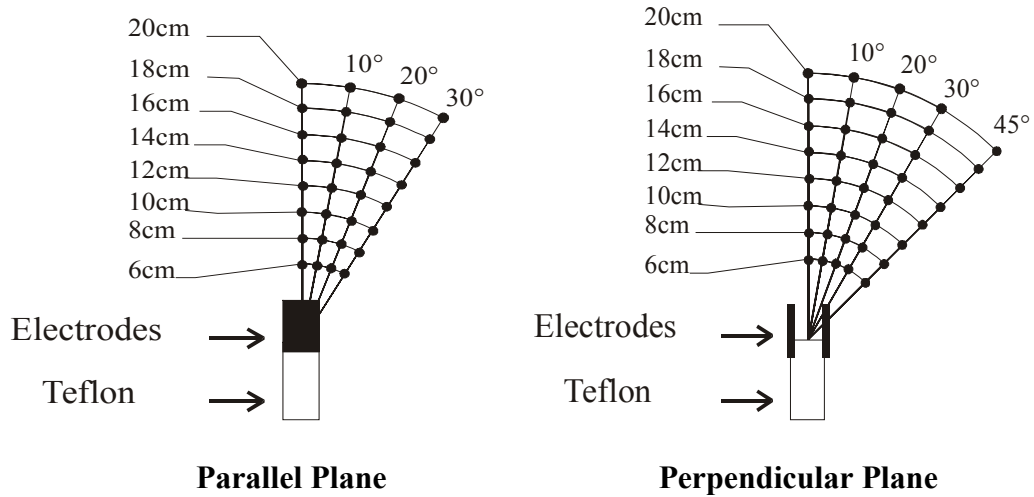


Figure 2.8: Measurement locations

For each set of measurements, the thruster was oriented to the correct angle. The probes were lined up using a plumb bob and template that fit on the exit plane of the thruster, moved vertically to a known location, and the tank was closed and returned to vacuum. The thruster was set to the appropriate energy level, E , initially 20 J, by setting the required voltage through $V = \sqrt{2E/C}$ given that $C = 33 \mu\text{F}$. At each angular position, five triple Langmuir probe measurements were recorded at locations 6, 8, 10, 12, 14, 16, 18 and 20 cm from the Teflon surface. Measurements could not be taken at 6 and 8 cm on the thruster centerline due to excessive electrical noise in the thruster discharge. After these 40 measurements were recorded, the probes were positioned exactly as they were for the first of this set of measurements. A final single pulse was recorded, and compared to the first measurement taken. This was done to alleviate concerns of probe contamination during a test cycle.

This data sampling procedure was repeated for 5 J and 40 J, with glow cleanings after each energy level. Our experiments resulted in 930 triple probe traces covering 62

positions for three energy levels. Each output trace from the probes was recorded, and stored for later analysis.

Chapter 3

Data Reduction, Analysis and Discussion of Results

In this chapter, triple Langmuir probe data and analysis is presented. This is accomplished by a series of smoothing algorithms and programs resulting in the electron temperature and density in the PPT plume over a range of radial and axial locations and thruster operating conditions. In addition, an effort is undertaken to investigate the cause of the two ion velocity populations as identified in earlier single Langmuir probe data [Eckman, 1998].

3.1 Triple Langmuir Probe Data Reduction and Analysis

Using the setup, diagnostics and procedures previously outlined in Chapter 2, triple Langmuir probe measurements were taken at various locations in the plume of a pulsed plasma thruster. The final experimental setup and data collection was performed in conjunction with Byrne and Cameron [1998], who performed preliminary data analysis on the collected results. Measurement locations are illustrated in Fig. 3.1, showing the angular locations θ_{\parallel} and θ_{\perp} in the parallel and perpendicular planes, respectively. For each of these angular locations, data was collected for five thruster firings at distances 6,

8, 10, 12, 14, 16, 18 and 20 cm from the Teflon surface. Each of these measurements resulted in a voltage and current trace from which the electron density and temperature can be found.

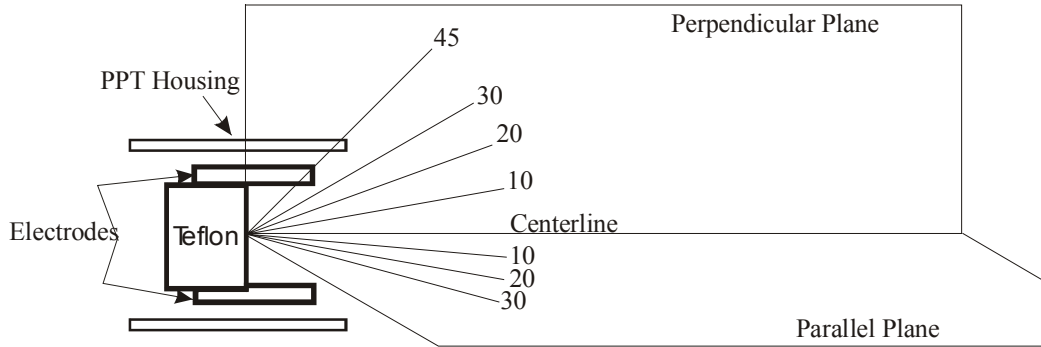


Figure 3.1: Measurement angles in parallel and perpendicular planes.

A typical set of voltage and current traces is shown in Fig. 3.2. Of particular interest in these measurements is the presence of noise. This manifests itself in two ways. Inherent in the PPT discharge is a short burst of electromagnetic noise at the start of the pulse, emitted as the spark plug breaks down the gap and initiates the discharge [Thomassen, 1973]. This noise can be seen on both the voltage and current traces, in the initial portion of the pulse. The second source of noise in the measurements is due to the signal processing of the voltage measurements. The signal from each probe input to the oscilloscope was digitally subtracted resulting in the measurement of a very small difference (~ 2 V) between relatively large voltages (~ 200 V). Because of the magnitude of the raw voltages being measured, a 10:1 voltage probe was used to reduce the signal to an acceptable level. The measured voltage differences were very near the lower accuracy bounds for the oscilloscope. When the true magnitude of the voltage difference was

recovered, by multiplying the signal by a factor of 10, the level of noise was also increased by an order of magnitude. This can be seen in the voltage trace in Fig. 3.2.

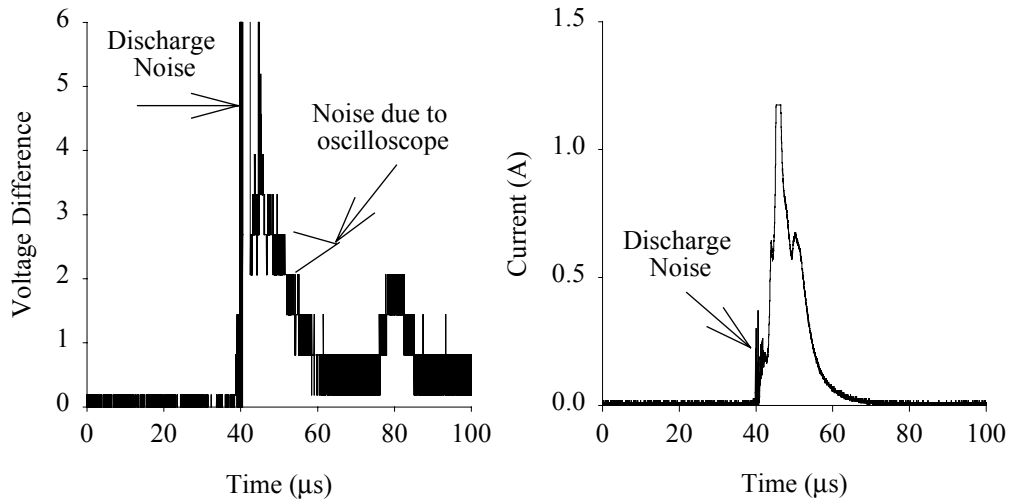
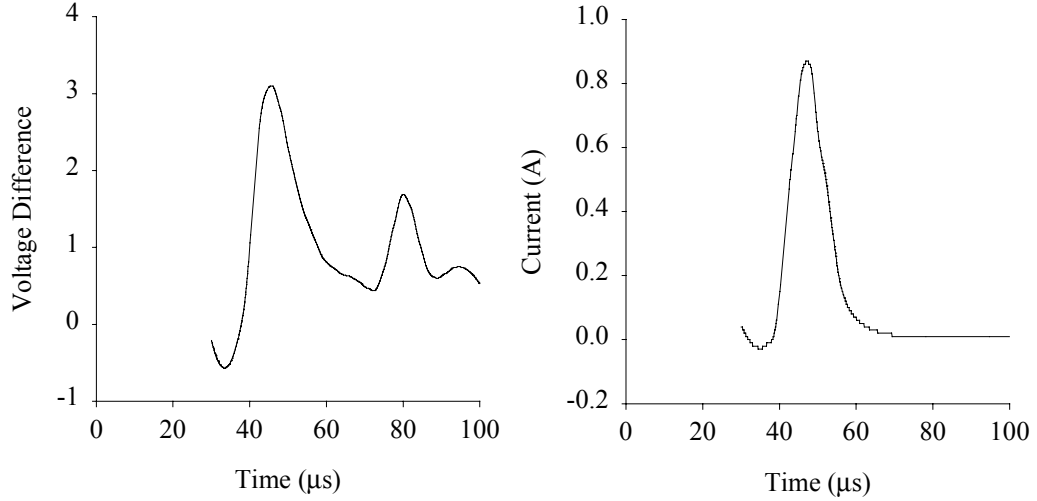


Figure 3.2: Raw voltage and current traces with descriptions of various noises.

The loess smoothing algorithm was applied to these traces, to reduce the noise using a statistical package S-Plus [MathSoft, 1997]. Loess smoothing works by taking a set number of neighbors around a certain data point. These points are averaged, with the points closer to the data point holding more weight in the average. The implementation of this method in S-Plus allows residual values to be reported, from which error bars can be generated. In the loess algorithm used to smooth the data, the span is 0.2, meaning that 20% of the data is considered for each data point and a second degree polynomial was generated for each local fit. The loess algorithm is applied to the current and voltage traces, typically resulting in smoothing shown in Fig. 3.3, which are smoothed examples of the data presented in Fig. 3.2.



**Figure 3.3: Smoothed voltage and current traces for 20 J centerline measurement
14 cm from Teflon.**

Using the smoothed voltage and current data, electron temperature and density is obtained using the theory outlined in Chapter 2. A brief outline of the algorithm used to obtain electron temperature and density is as follows:

1. Use thin sheath approximation to find T_e , n_e from Eqs. 2.5 and 2.10.
2. Calculate Debye length $\lambda_D = \sqrt{\epsilon_o T_e / en_i}$ using T_e , $n_i \cong n_e$
3. Calculate α , B from curve fit of Laframboise results from Eqs. 2.13 and 2.14.
4. Find floating potential χ_f using Eq. 2.18.
5. Use χ_f to find η , β using Eqs. 2.16 and 2.17.
6. Find T_e and n_e using Eqs. 2.19 and 2.20
7. Loop to step 2, iterate until T_e converges.

The Fortran program written to handle the data conversion is included in Appendix I. The code was validated by entering voltage and current data reported for a

triple Langmuir probe study on an arcjet [Bufton et al., 1995]. The result of this procedure provides the time evolution of electron temperature and density at a specific location, and a typical sample from a 20 J centerline pulse 14 cm from the thruster is shown in Fig. 3.4. It is important to note that the time scale on these plots does not begin at a specific event, but that they do correctly show the passage of time and the duration of the pulse.

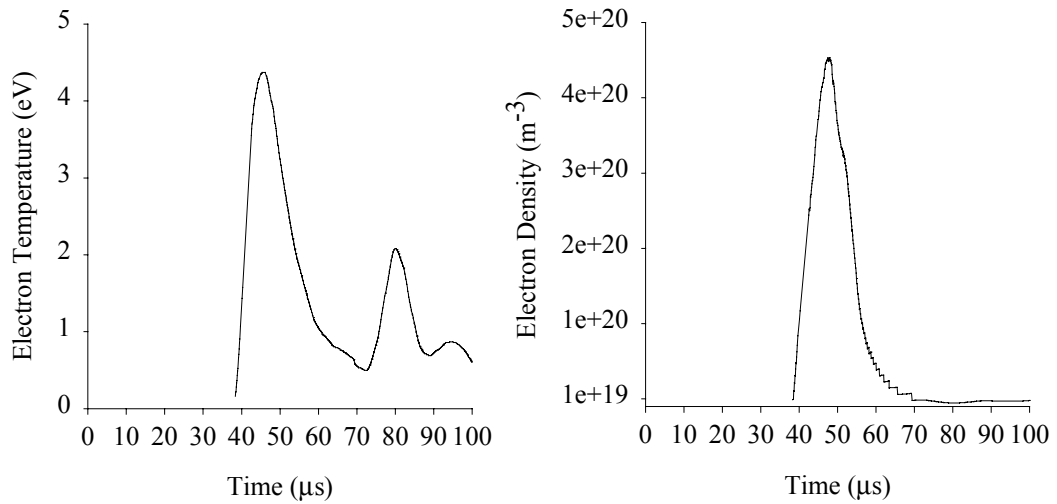


Figure 3.4: Sample T_e, n_e curves for 20 J centerline, 14 cm from Teflon.

What follows is an analysis of electron temperature and density PPT plume as a function of location, thruster energy level, and measurement plane. Maps of maximum density and bulk electron temperature summarize the overall picture of temperature and density in the plume, showing overall temperature and density variation as the plume expands from the thruster.

3.1.1 Error Analysis

In our experiments there are several potential sources of error due to the probe theory and also due to the methods used to obtain the data. The error in T_e measurement using a triple probe in the proper operating regime has been estimated to be approximately 15% and the failure of the condition $Kn_{ii} \gg 1$, as discussed in Chapter 2, is not expected to increase this error [Tilley et al., 1990]. The voltage probes and oscilloscope used to record V_{d2} introduced a high frequency noise into the measurements, on the order of ± 0.75 eV, which was smoothed during data reduction, as described below. The main error in n_e estimates is due to the fact that $Kn_{ii} \sim 1$, as discussed above and this introduces an error of $\sim 60\%$ [Tilley et al., 1990]. There was a minimal amount of noise in the current measurements and the effect of the voltage noise introduced a $\pm 10\%$ uncertainty into the density measurements.

Error bars due to smoothing are plotted in Fig. 3.5. In Fig. 3.6, these same error bars are compared against the error due to probe theory. In the temperature plot, the larger error bar is due to smoothing, while in the density plot, the larger bar is due to probe theory and so it is evident that in the temperature measurements error due to smoothing predominates, while in the density measurements error due to the violation of the ion free molecular flow assumption is the largest.

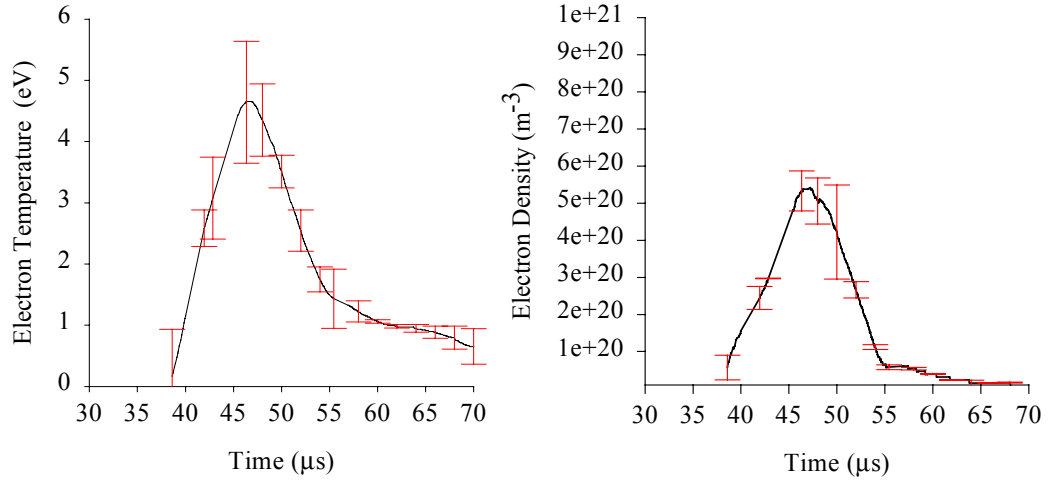


Figure 3.5: Error in T_e , n_e due to smoothing.

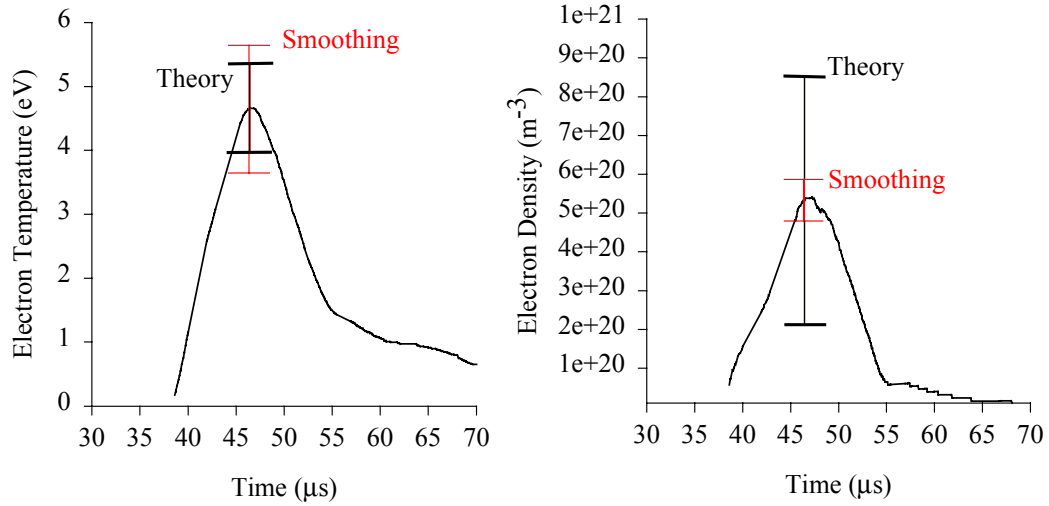


Figure 3.6: Comparison of smoothing and theory error.

The spatial resolution of the probes is related to the total volume taken by the probe tip. For our case, the probe volume is a cylinder with a diameter of 2 mm and a length of 9 mm. All spatial locations reported are measured to the tip of the probe wires. The probe tip was observed to vibrate during testing, due to the backing pump attached to

the oil diffusion pump. This vibration was estimated to be approximately 1 cm in each direction, and this distance defines the spatial accuracy of these measurements.

It was mentioned previously that for the off centerline locations, the probe was aligned geometrically with the center of the Teflon surface. This may result in a probe misalignment with the flow vector, which may not line up with the geometric vector. To correctly apply the theory derived above, the probes should be aligned with the flow vector, and so a study must be done at each measurement location to determine the proper positioning of the probe. In an MPD thruster plume, however, it was found that triple probes may be misaligned with the flow by as much as 30 degrees before any significant error in measurement occurs [Tilley et al., 1990]. In the present measurement locations, it is assumed that this criteria is met.

3.1.2 Electron Temperature and Density of PPT Plume

Figure 3.7 shows the sample electron density and electron temperature traces for the 20 J case for $r_{\perp} = 6, 12, \text{ and } 20 \text{ cm}$ at $\theta_{\perp} = 10 \text{ degrees}$. The maximum and minimum density and temperature traces are plotted for each location, showing the unsteady character of the PPT plume as it passes by the triple probe. Simultaneous electron temperature and density for a 20 J pulse measured $r_{\perp} = 12 \text{ cm}$ and $\theta_{\perp} = 10 \text{ degrees}$ is plotted in Fig. 3.8. From this plot, it is seen that the highest electron temperature for each spatial location occurs at the beginning of the pulse, when the most energetic electrons leave the thruster, while the highest density occurs near the middle of the pulse. In some of the electron temperature traces, there is apparently a secondary peak after the plasma passes the probes. There is no corresponding density increase at this time, and it was

concluded that this peak is due to electrical noise or grounding problems in the probe apparatus. It should be noted that this is not expected to impact the evaluated data.

3.1.3 Spatial Variation of Temperature and Density

To evaluate spatial trends in the expansion of the PPT plume, it is convenient to concentrate our analysis on maximum electron density measured at each location. In the spatial analysis of the data, the maximum density n_e^{max} for a single trace is recorded at a location (r, θ) , and the time at this is measured is denoted as t^* . The electron temperature T_e^{bulk} at t^* is recorded as well, as illustrated in Fig 3.8. This procedure results in five maximum electron density values and their related electron temperatures. These data are averaged for a single location, producing the values N_e^* and T_e^* , representing the average maximum electron density and the average electron temperature at t^* . Plotting N_e^* and T_e^* over a range of values for r results in the trend lines plotted in Fig 3.9.

During experimentation, it was found that there was some degree of variation in the electron density and temperature measurements on a pulse to pulse basis. The centerline density and temperature variation is plotted for the 20 J, centerline case in Fig. 3.9. To account for the pulse-to-pulse variation in $n_e^{max}(r, \theta)$ and $T_e^{bulk}(r, \theta)$ a measure of the spread of these values is obtained. The average range of $n_e^{max}(r, \theta)$ is $\pm 41\%$ of N_e^* for the 5 J case, $\pm 43\%$ for 20 J and $\pm 47\%$ for 40 J. The average range for $T_e^{bulk}(r, \theta)$ is $\pm 23\%$ of T_e^* . As discussed earlier, for all measurements the uncertainty in $n_e^{max}(r, \theta)$ is estimated to be $\pm 60\%$, the uncertainty in $T_e^{bulk}(r, \theta)$ is ± 0.75 eV and the spatial accuracy is ± 1 cm.

Figure 3.10 shows the axial variation for the 5 J PPT. The N_e^* decreases with increasing distance in both the parallel and perpendicular plane. Temperature T_e^* is larger close to the exit and decreases as the plasmoid expands. The angular variation is also

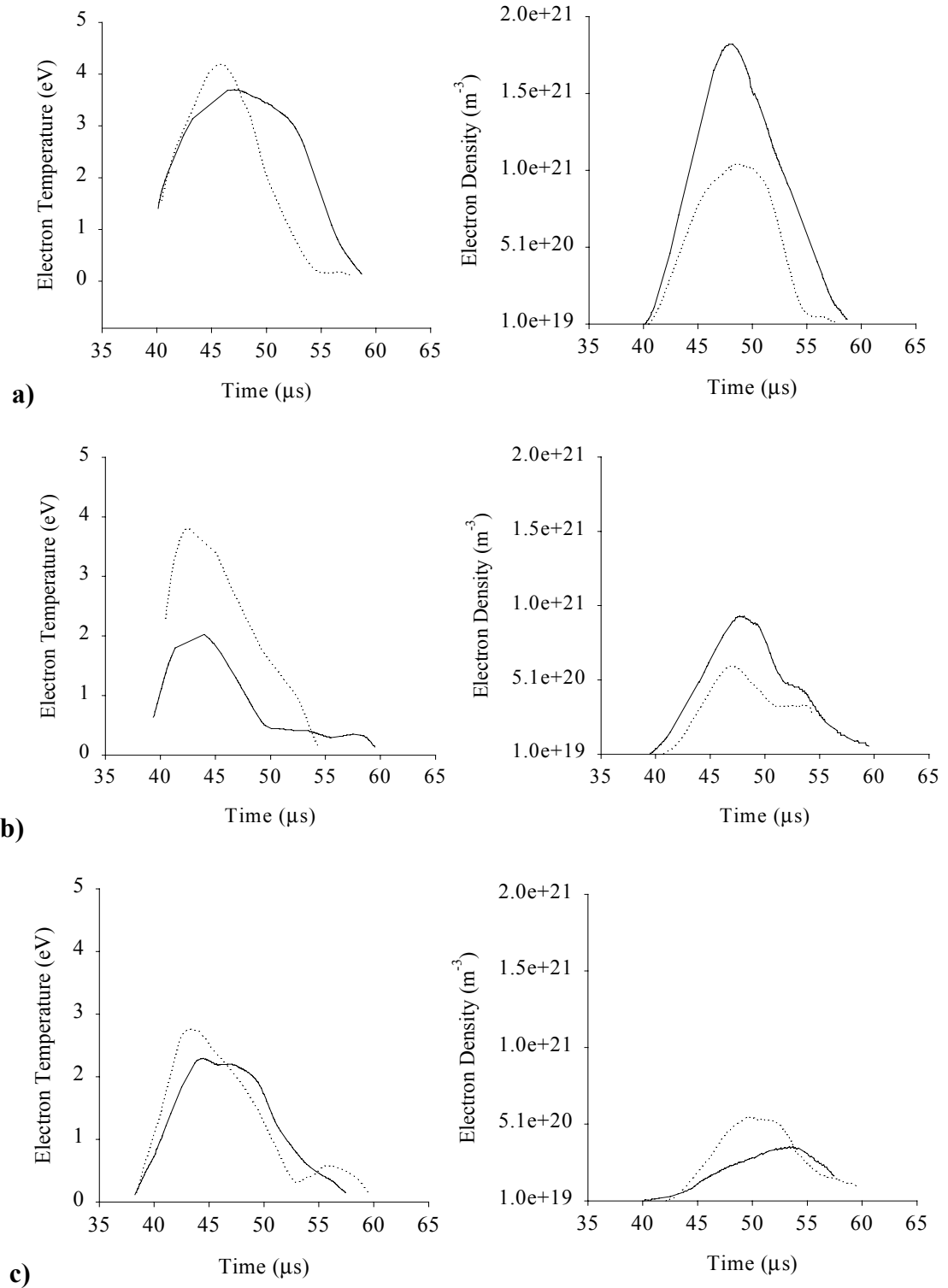


Figure 3.7: Smallest and largest peak value traces for: a) $r = 6$ cm, b) $r = 12$ cm, c) $r = 18$ cm.

c) $r=18$ cm, 10 degrees off axis in the plume of a 20J PPT.

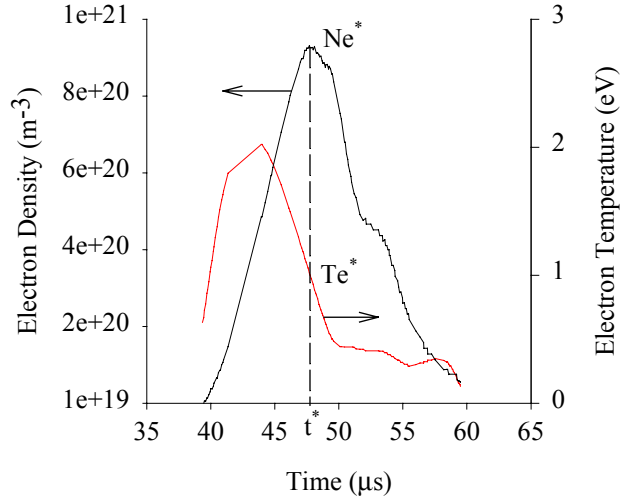


Figure 3.8: Electron temperature and density measurement in a PPT plume.

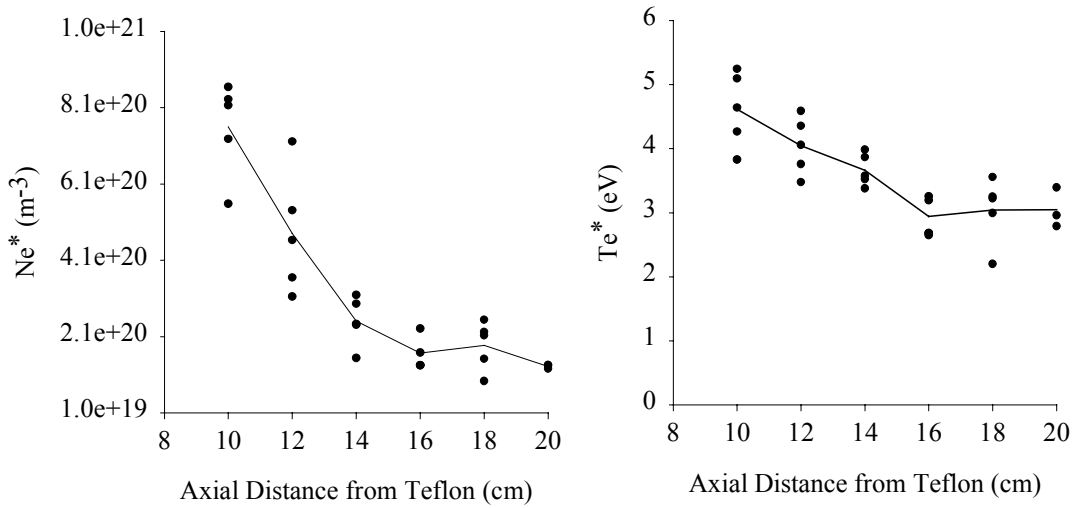


Figure 3.9: Per Pulse N_e^* and T_e^* along centerline in a 20 J PPT plume.

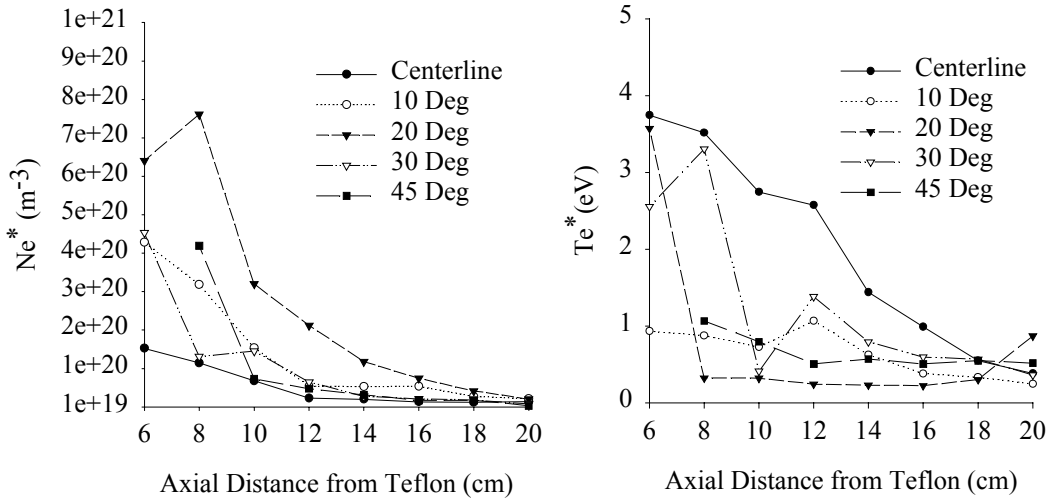
depicted in Fig. 3.10. The perpendicular plane shows considerable angular variation in both density and temperature. However the parallel plane does not show any

considerable variation as Fig. 3.10.b depicts. This is a direct result of the configuration of the LeRC PPT shown in Fig. 2.1, where acceleration mechanisms are expected to be almost uniform in planes parallel to the electrodes. From the cross section of the thruster with measurement angles shown in Fig. 3.1 it seen that in the perpendicular plane the plume is much more confined than in the parallel plane, possibly causing the non-axisymmetric nature of the plume. Temperature in the perpendicular plane is highest along the centerline as expected. Our data fail to show a monotonic decrease with increasing angular position for all axial positions.

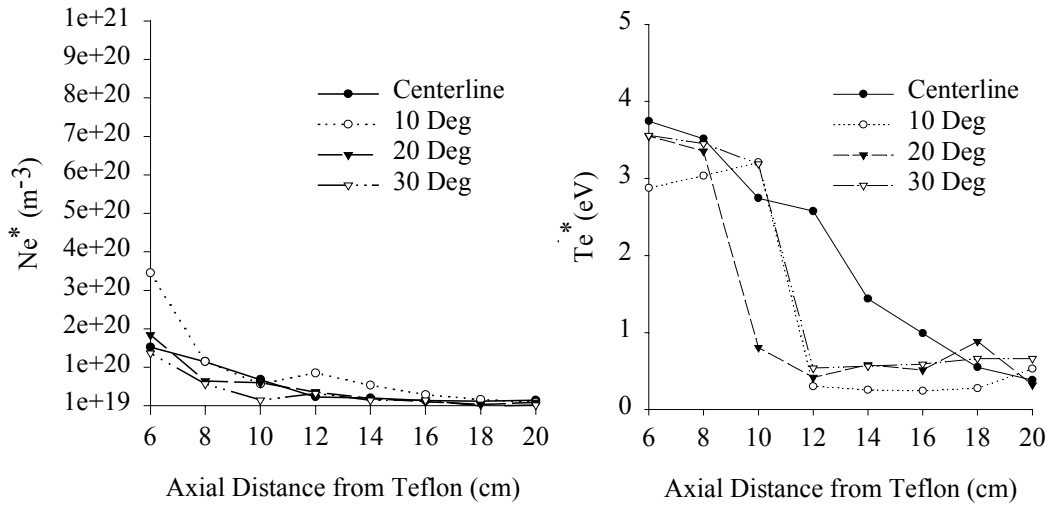
Fig. 3.11 shows N_e^* and T_e^* trends for the 20 J energy level. Density in the perpendicular plane decreases as a function of axial distance. In addition, density decreases monotonically with increasing angular position for most part of the plume, as Fig. 3.11.a shows. As axial distance increases the difference between densities in the two planes becomes approximately a factor of four, values within our experimental error. Temperature along the centerline is approximately 5 eV and is almost constant as Fig. 3.11.b shows. Off-axis T_e^* are lower and become approximately 1 eV for both the parallel and perpendicular planes. As with the 5 J case, variation of density in the parallel plane is not significant. However electron temperature is highest along the centerline, and decreases monotonically with angular position as Fig. 3.8.b shows. Density in the parallel plane decreases from $N_e^*(r_{\parallel} = 6cm) \cong 1.5 \times 10^{21} m^{-3}$ to $N_e^*(r_{\parallel} = 20cm) \cong 2 \times 10^{20} m^{-3}$. The temperature in the parallel plane shows considerable angular but little axial variation.

Figure 3.12 shows N_e^* and T_e^* variation for the 40 J energy setting. These plots show similar trends as the 5 and 20 J cases. Density shows angular variation in the

perpendicular plane but not in the parallel as a comparison between Fig. 3.12.a and Fig 3.12.b shows.

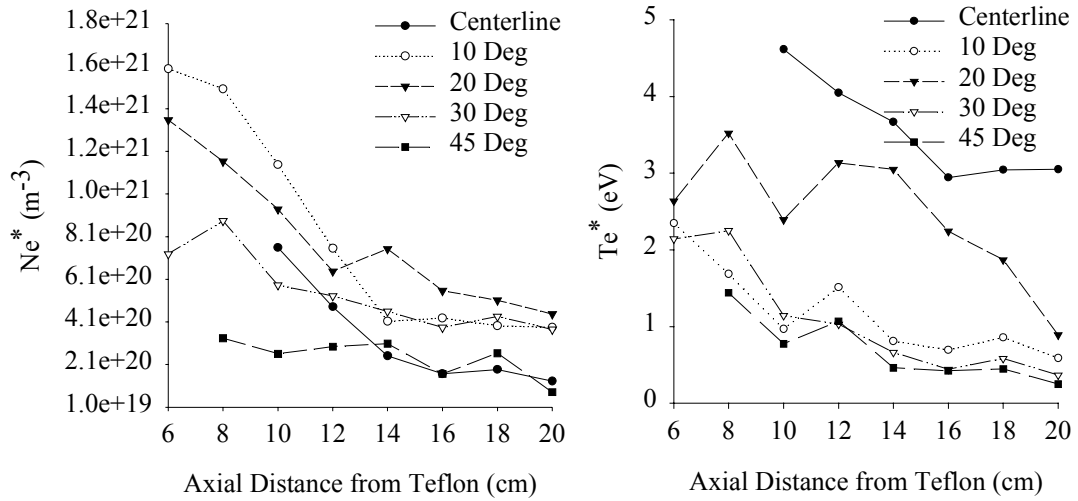


a) Perpendicular plane

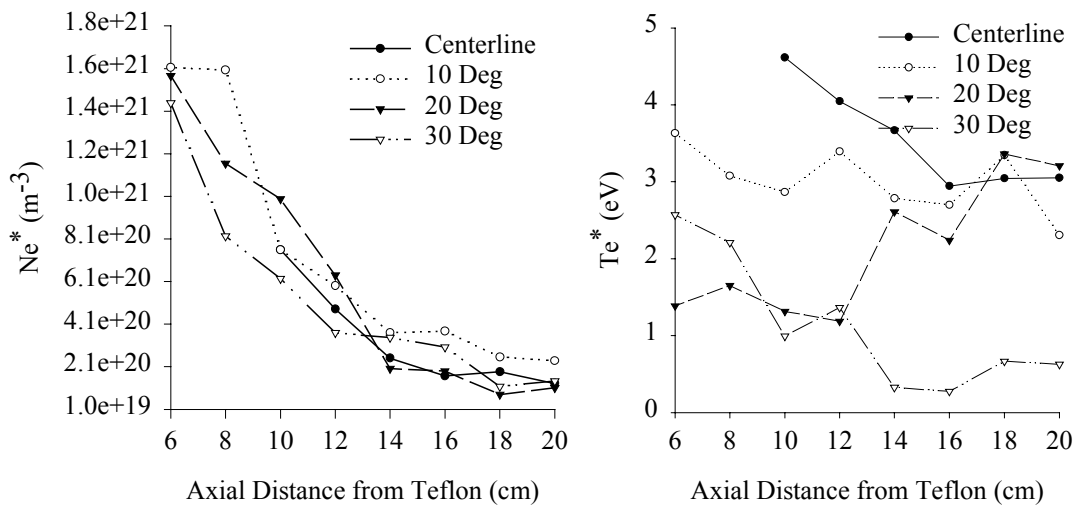


b) Parallel plane

Figure 3.10: Spatial variation of N_e^* and T_e^* in a 5 J PPT plume.

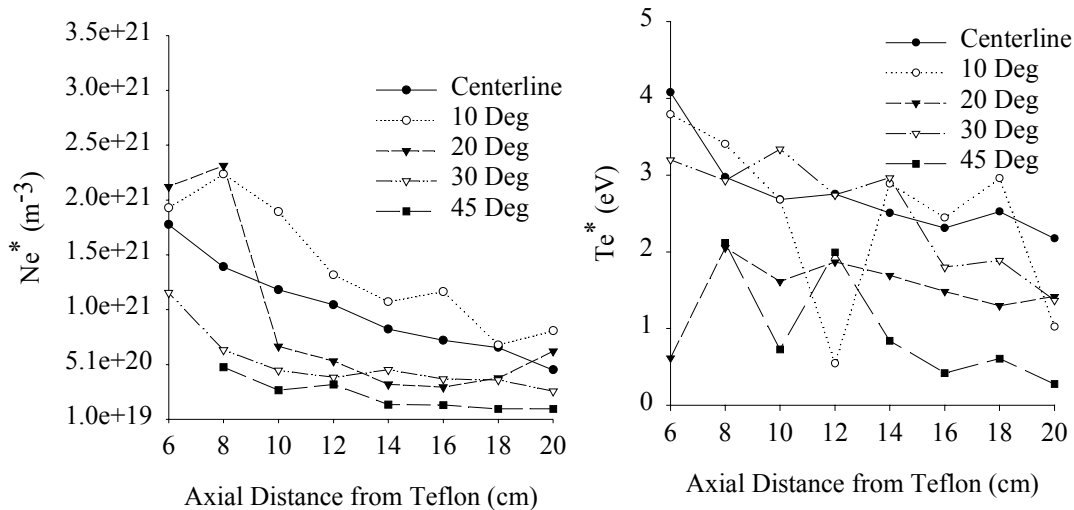


a) Perpendicular plane

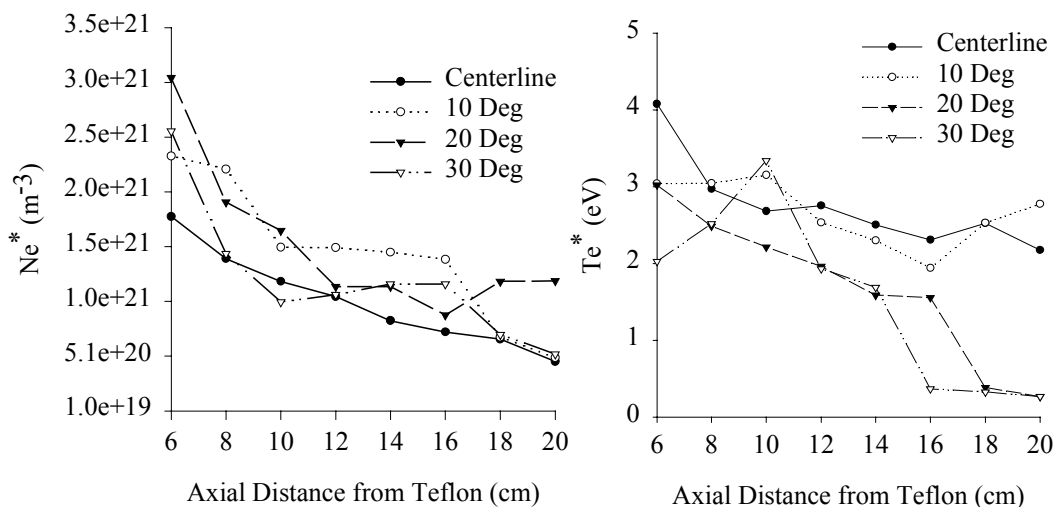


b) Parallel plane

Figure 3.11: Spatial variation of N_e^* and T_e^* in a 20 J PPT plume.



a) Perpendicular plane



b) Parallel plane

Figure 3.12: Spatial variation of N_e^* and T_e^* in a 40 J PPT plume.

3.1.4 PPT Discharge Energy Effects

The spatial variation of the plume shows how electron temperature, T_e^* and density, N_e^* at t^* can be summarized to show the effect of discharge energy. Figure 3.13 shows N_e^* and T_e^* along the centerline for all three energy levels as the PPT is throttled. The density N_e^* shows an order of magnitude increase as the thruster is throttled from 5 to 40 J. This corresponds to an increase of impulse bit of nearly 14 times between these two settings as Table 2.1 shows. The plots also show an overall lack of change in electron temperature T_e^* as a function of energy level, especially very near the thruster exit.

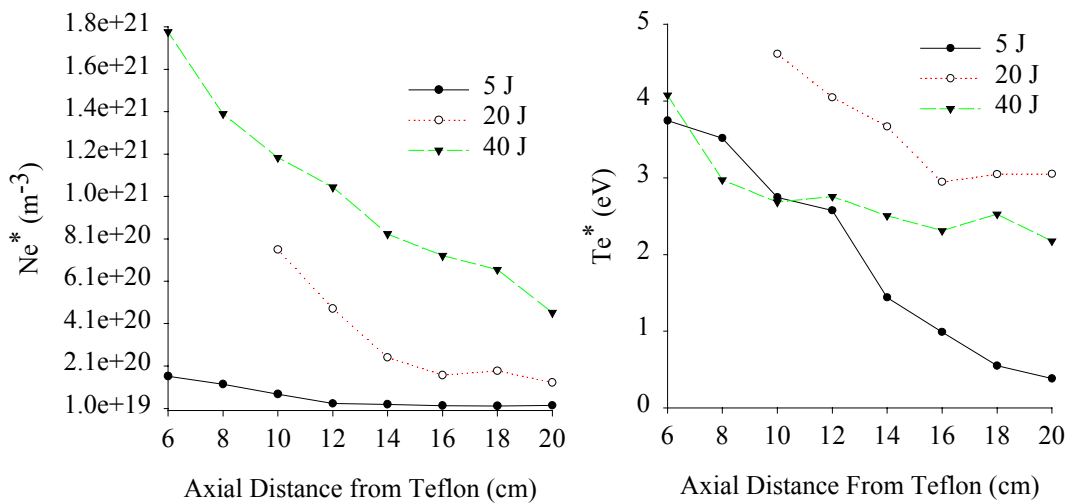


Figure 3.13: Spatial variation of N_e^* and T_e^* along centerline in 5J, 20J, and 40J PPT plume.

3.2 Single Langmuir Probe Data Analysis

In previous work at NASA Lewis, ion speed data was estimated based on single Langmuir probe data collected in a 3 x 1 meter vacuum chamber. A detailed description of these experiments can be found elsewhere [Eckman and Santesson, 1996, Eckman et al., 1998] and is summarized here. In this experiment, the LES 8/9 flight hardware was used to generate the plume. This thruster runs at 20 J, and has nearly identical characteristics to the LeRC-PPT at 20 J, ablating 28.5 μg of Teflon per pulse, and having an impulse bit of 300 $\mu\text{N}\cdot\text{s}$. To measure the speed of ions in the plume of the PPT, two collinear single Langmuir probes were used. These probes were biased negatively with respect to the plume, and as the plasma passed, ion current was collected by each probe as shown in Fig. 3.14 for a typical case. The traces from each probe were recorded simultaneously, and from these traces the speed of the ions could be calculated using $V = D/T_f$ where $D=0.15$ m is the distance between the probes and T_f is the time for each wave to travel between the two collinear probes. Ion velocity plots are shown in Fig. 3.15 for both ion populations.

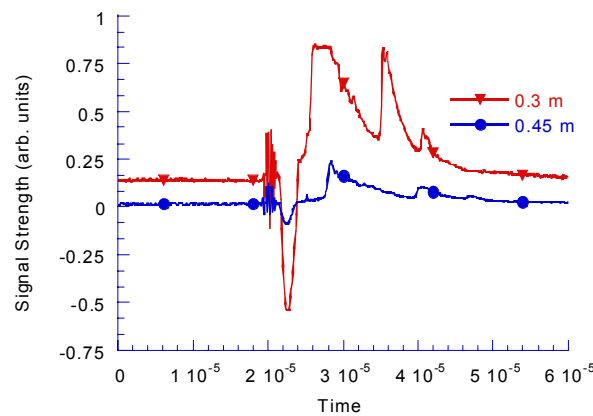


Figure 3.14: Sample single Langmuir probe traces.

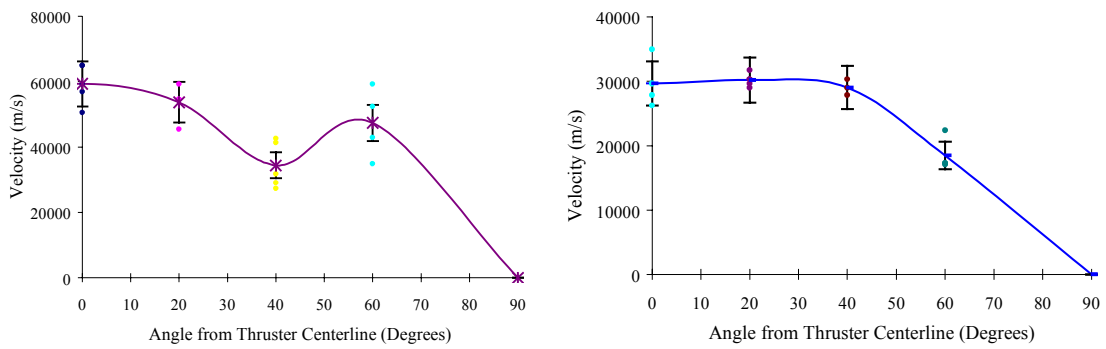


Figure 3.15: Fast and slow ion population velocities.

From this analysis, two characteristic ion populations were identified in each single Langmuir probe trace, a slow one traveling at about 30 km/s and a faster one traveling at approximately 60 km/s. There are several possible causes for this observation, relating to processes during the discharge inside the thruster. The first possible cause is known as the slug-restrike mode of thruster operation. In this mode, the arc forms and accelerates down the channel with the plasma, continually accelerating the plasma blob. At some point, the arc restrikes at the face of the Teflon and stands at this location for the remainder of the discharge. Ions propelled in this phase of the discharge would experience less acceleration, since they are under the influence of electromagnetic acceleration for a shorter period of time. Another possible cause of the multiple ion velocities is the presence of multiply ionized, and therefore faster, species in the plume. A third possible cause is the segregation of masses that results in faster velocities for lighter plume species.

To better understand the creation of these separate ion velocities, the difference in creation time between these two populations was studied, based on the previously

obtained single Langmuir probe traces. Using this data, and assuming that the velocity of the ions does not change as they move downstream of the thruster, the difference in creation time can be found, using the relation:

$$\Delta t_c = x \left(\frac{1}{V_1} + \frac{1}{V_2} \right) + \Delta t_m \quad (3.1)$$

where Δt_m is the time for the pulse to travel between the two probes, x is the distance to the first probe, V_1 and V_2 are the velocities of the first and second waves and Δt_c is the difference in wave creation time. Considering measurements on the centerline and 20 degrees off of centerline, where the measurements are easiest to interpret, the resulting Δt_c are shown in Table 3.1.

0° from C.L.	20° from C.L.
Δt_c (μ s)	Δt_c (μ s)
1.89	2.92
2.89	4.23
1.49	2.58
5.17	3.01
3.98	3.94
Average: 3.08	3.33
Average $\Delta t_c = 3.20 \mu$ s	

Table 3.1: Average time difference between creation of ion populations.

From this result, it is possible to eliminate mass segregation as the source of the dual wave nature. If this were the case, then the waves would appear to be created simultaneously. The difference in creation time seems to follow the oscillating discharge waveform. A characteristic of the PPT discharge is a voltage and current reversal about 3 μ s after the discharge initiation as shown in Fig 3.16 for a typical case for the LES 8/9 PPT [Thomassen, 1973]. The discharge continues to oscillate several times, although with a much lower magnitude than the first peak and trough.

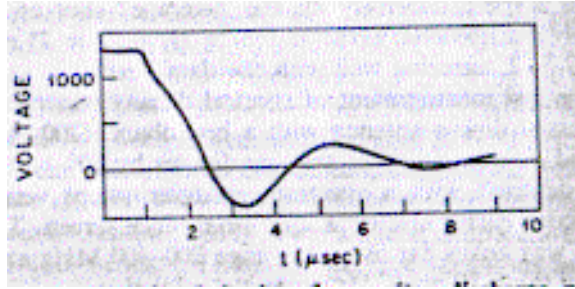


Figure 3.16: Sample LES 8/9 voltage discharge, [Thomassen, 1973].

It is therefore possible that faster, multiply ionized particles are created in the initial, high current arc. The “trough” in the oscillation, which would correspond to the second “wave” of ions, is actually a negative voltage, resulting in a current flow in the opposite direction. This second current peak may not have enough energy to create as many multiply ionized particles, and thus the second wave of ions could be primarily singly ionized particles. This conclusion can be correlated by spectroscopic observations of the PPT discharge, which show that as the discharge current oscillates and decays, it is able to create lesser amounts of multiply ionized particles with each fluctuation [Markusic et al., 1997].

Chapter 4

Summary, Conclusions, and Recommendations

In this thesis, electron temperature and density measurements were taken in the plume of a pulsed plasma thruster. Triple Langmuir probes were used to collect data over a wide range of downstream positions and for three discharge energy levels. These probes have the ability to instantaneously record electron temperature and density, and have the benefit of being relatively simple to use, compared to other methods used to measure these same properties. The implementation of this measuring technique is discussed in detail, to aid future work that utilizes these devices. In addition, analysis of single Langmuir probe data collected in the PPT plume was performed. This analysis estimated the length of time between the creation of the two ion populations observed in the PPT plume, and provided possible causes for this phenomenon. These results and conclusions are summarized in detail below, followed by recommendations for future work.

4.1 Summary of Experimental Setup, Diagnostics and Procedures

Triple Langmuir probes were used to obtain electron temperature and density measurements in the plume of a NASA Lewis laboratory model pulsed plasma thruster. These probes have been used in the plumes of electric propulsion devices previously, but never in the pulsed plume of the PPT. Previous attempts by WPI researchers at using triple probes in the PPT plume had excessive noise and grounding problems. To solve the noise problem, the probe circuitry was altered and a differential amplifier used in previous studies was removed. Instead, voltage differences were computed digitally on an oscilloscope. Additionally, the experimental setup was electrically isolated from the vacuum chamber and a common ground was used for all electronics and measurements. The combination of these two tactics seemed to provide the best setup for taking measurements with the triple probes.

A computer-controlled probe translation system was built to allow the axial movement of the probes without venting the vacuum facility. This allowed for a greater amount of data to be collected in a relatively short time span. A glow discharge probe cleaning apparatus was built and attached to the probe rake near the probe tips. During experimentation the probes were routinely cleaned to remove contamination built up on the probe electrodes. The theory used to obtain electron temperature and density from the probe output was reviewed and calculations were made to ensure that the theory is applicable to the plume being measured.

4.2 Summary of Data Reduction, Analysis and Results

4.2.1 Triple Langmuir Probe Data Reduction

Plasma measurements were taken at 6, 8, 10, 12, 14, 16, 18 and 20 cm from the face of the Teflon fuel bar along the centerline, and at 10, 20 30 and 45 degrees off of centerline in the planes parallel and perpendicular to the thruster electrodes for thruster energy levels of 5, 20 and 40 J. There was a significant amount of noise in the measurements, due to electromagnetic interference from the thruster discharge and the precision with which the oscilloscope could record data. This second source of noise was introduced by correcting for the voltage probe that was used to reduce the collected voltage to a measurable level. To smooth out both of these sources of noise the loess smoothing algorithm was applied to the data. The pulse to pulse variation of the thruster was examined, showing that density varied by up to 50% and temperature varied by up to 25% on a single pulse basis. Simultaneous electron temperature and density measurements show that the hottest electrons populate the leading edge of the pulse, and that the temperature of the densest portion of the electrons is slightly lower than the maximum temperatures recorded in the plume.

4.2.2 Error Analysis

An error analysis was performed on the triple Langmuir probe measurements. For the densities being measured, the $Kn_{ii} \gg 1$ condition required by the probe theory does not hold, and previous investigators have estimated that this introduces an error of 60% in the electron density measurements. The error for electron temperature measurements has been estimated in literature to be 15%. These errors are in addition to

the uncertainty generated due to the initial smoothing of the data traces. Error bars due to smoothing are generated from the residual values of the loess algorithm, and for the electron temperature measurements this uncertainty is approximately ± 0.75 eV. The uncertainty due to smoothing of the density measurements is approximately $5 \times 10^{19} \text{ m}^{-3}$. It can be concluded that for the electron temperature measurements the largest source of error is due to the smoothing of the traces. For the density measurements the $\pm 60\%$ uncertainty from the theory is much larger than the error due to smoothing.

4.2.3 Results and Discussion

Five measurements were recorded at each of the locations listed above, and these measurements were averaged to show trends in the data. To analyze the expansion of the plume the average maximum density and the average temperature that occurs at maximum density were plotted for various energy levels, showing the plume axial and radial variation of the plume.

For 5 J discharges, maximum electron densities range from 1×10^{19} to $7 \times 10^{20} \text{ m}^{-3}$ over the range of measurement locations and bulk temperatures range between 0.5 and 3.75 eV. A thruster energy setting of 20 J shows peak density ranging between 1.6×10^{21} and $1 \times 10^{20} \text{ m}^{-3}$ and temperatures ranging between 0.5 and 4.5 eV. The 40 J case has the highest densities, as is expected, with a density range of 1×10^{20} and $3 \times 10^{21} \text{ m}^{-3}$ and bulk temperatures between 0.5 and 4.0 eV. The plume densities and temperatures are highest near the thruster, as would be expected. The smallest measured values were taken on the fringes of the plume, at 30 and 45 degrees from the plume centerline.

From the plots of temperature and density, several trends emerge. For all energy levels, the perpendicular plane shows much more radial variation than the parallel plane.

This can be attributed to the rectangular geometry of the electrodes in the thruster nozzle. These measurements confirm the non-symmetric nature of the PPT plume, which is a very important consideration in plume/spacecraft interaction studies. The addition of a horn type nozzle as seen on the LES 8/9 and EO-1 thrusters may serve to make the plume more axisymmetric although experimentally this is unconfirmed.

Bulk electron temperature generally shows a decrease of about 1 eV as the plume expands from 6 to 20 cm from the Teflon surface. There is not a significant difference in electron temperatures between the energy levels, with the exception of the 5 J plume, where the temperatures drop off faster axially than in the higher energy discharges. Near the thruster exit, however, bulk temperatures are nearly equal for all energy levels. The shot-to-shot variation of the plume density was examined for the centerline measurements for the 20J case. There is, at maximum, a 50% density variation from mean on a shot-to-shot basis while electron temperature shows a maximum variation of approximately 25%.

4.3 Summary of Ion Velocity Results

Previous experiments at NASA Lewis Research Center using single Langmuir probes in the plume of a PPT had identified two ion velocity populations of 30 and 60 km/s respectively. In an effort to gain an insight into the processes during the thruster discharge further analysis was performed on this data to estimate the creation time of each of these populations. Using the velocity of each population and assuming that the velocity did not change over the course of the ion time-of-flight, the difference in creation time was found to be approximately 3 μ s. This time corresponds almost exactly with one half of the period of the PPT discharge oscillation, suggesting that as the

discharge voltage and current oscillate, different ion populations formed. This conclusion could also be correlated by spectroscopic observations of the discharge in the PPT channel which observe the creation of doubly ionized species during the first discharge oscillation and predominantly singly ionized particles in the second oscillation.

4.4 Recommendations for Future Work

Recommendations involve improvements in the circuitry and equipment used in our experiments as well as with measurement techniques and locations that would provide further insights into the PPT plume.

- **Improve Batteries used in Circuitry**

There is concern that the 9 V batteries used cannot handle the current of around 1 A that is recorded in the highest density measurements. A larger battery capable of handling a higher load would be desirable, to assure that this does not have any adverse effect on the measurements.

- **Improve Recording Methods**

Equally important would be a better method of recording the voltages required for the triple probe measurements. The problem with these measurements is the fact that a very small difference was being measured between two very large voltages, which required a low resolution setting on the scope to capture these two large signals. An oscilloscope that was capable of handling larger input voltages would most likely reduce or entirely eliminate the noise introduced from the oscilloscope.

- **Trigger Measurements from Common Event**

When the present set of data was recorded, the recordings were triggered by the arrival of the signal itself. This method does not allow the spatial and temporal

development of the plume to be examined, since the time scale on the traces represents only the passage of time. A method of triggering the recording off of some common event should be found. This would allow, for instance, time-of-flight calculations to be made with only one probe that could take measurements at several locations. The trigger must have a high degree of accuracy and repeatability, and ideally should be repeatable to within only a few microseconds to properly capture the plume movement downstream.

- Record Measurements in Backflow Region

The current set of data only includes downstream measurements in the core of the PPT plume. Measurements in the backflow area of the PPT are of great importance, because they reveal information about possible plume/spacecraft interactions. The densities measured at the 45 degree from centerline positions in this study were at the lower range of detectable levels for the equipment that was used. To obtain a detectable signal in the backflow region, the sensitivity of the measuring devices would need to be increased by at least an order of magnitude.

Appendix I

Computer Code

This Appendix contains all code used for data processing and analysis, including batch code used to initialize the data, the smoothing algorithms and the FORTRAN code used to reduce the data to electron temperature and density values. The following software programs were used for various parts of this work:

- WinBatch, by Wilson WindowWare. This is a batch program language for Windows, and was used for simple processing of large amounts of files. This program can be found at www.windoware.com.
- S-Plus 4.5, by MathSoft. This is a powerful statistical analysis package that was used to loess smooth the data. Information on this program can be found at www.mathsoft.com.
- Digital Visual Fortran, by Digital. This is a FORTRAN compiler for Windows 95 and NT, using Microsoft's Developer Studio interface. Information on this program can be found at www.digital.com/fortran.

A.1 Data Conversion Batch File

This WinBatch program converts the raw oscilloscope data files into ASCII text for the current and voltage measurements. It then generates a time scale, and combines the two data files with this time scale to produce a single comma separated data file for a particular measurement.

```
;To reduce files automatically
;This batch file takes the raw data files, uncompresses them
;creates an appropriate time scale, and combines all files into one
;comma delimited file.

;

curdir = DirGet()

FileCopy("e:\reckman\thesis\experimental    data\utilities\wavetran.exe",
curdir, @FALSE)
FileCopy("e:\reckman\thesis\experimental    data\utilities\lecroy21.tpl",
curdir, @FALSE)

StartFileNum = Askline("Start File Number", "Enter Start File Number",
"") ;Starting File Number
EndFileNum = Askline("End File Number", "Enter End File Number",
"");Ending File Number
Disk=Askline("Disk?", "What disk letter is this?","") ;Disk Letter

    curmul = Askline("Current Multiplier", "Enter Current Multiplier
in A/V","")
    curmul = curmul + 0.0
    volmul = 10.0
    timescale = Askline("Time Scale", "Enter Time Scale in usec/div",
"")

For number = StartFileNum to EndFileNum

    numstr = StrCat("0", number)
    numlen = StrCharCount(numstr)
    if numlen < 3
        numstr = StrCat("0", numstr)
    endif

    RunWait("wavetran.exe", "-tlecroy21.tpl -o%Disk%%numstr%VD2.dat
STA.%numstr%")
    RunWait("wavetran.exe", "-tlecroy21.tpl -o%Disk%%numstr%I.dat
SC2.%numstr%")
Next

;now add time scale, convert data using appropriate multipliers, and
combine to form single file
```

```

For number = StartFileNum to EndFileNum

    numstr = StrCat("0", number)
    numlen = StrCharCount(numstr)
    if numlen < 3
        numstr = StrCat("0", numstr)
    endif

;Open current files up

    outhandle = FileOpen("%Disk%%numstr%.dat", "write")
    vd2handle = FileOpen("%Disk%%numstr%VD2.dat", "read")
    ihandle   = FileOpen("%Disk%%numstr%.I.dat", "read")

;Prompt for current multiplier, time scale

;Now loop on time

    For i = 1 to 1000*timescale
        tim = (i-1) * 0.01
        vd2 = FileRead(vd2handle)
        vd2 = strtrim(vd2) * volmul
        cur = FileRead(ihandle)
        cur = strtrim(cur) * curmul
        FileWrite(outhandle, strcat(tim, ",", vd2, ",", cur))
    Next

    FileClose(outhandle)
    FileClose(vd2handle)
    FileClose(ihandle)

;    now clean up files not needed any more
    FileDelete("%Disk%%numstr%VD2.dat")
    FileDelete("%Disk%%numstr%.I.dat")
    FileDelete("sc2.%numstr%")
    FileDelete("sta.%numstr%")

    Beep

Next

beep
beep
Message("Complete",      "Batch      Processing      for:@CRLF%Disk:
%Disk%%@CRLF%Records: %StartFileNum% to %EndFileNum%")

```

A.2 S-Plus Smoothing Script

The following script takes a set of data files generated by the previous batch file and loads them into S-Plus. The files are then trimmed of leading blank spaces, and the amount of data points is reduced to decrease the file size and to expedite processing. The

loess algorithm is run on the current and voltage data, and the results, along with the appropriate error bars, are saved to disk as a comma separated ASCII file.

```

prefix <- "j"
exten <- ".dat"
startnum <- 16
endnum <- 52

energy <- "5J"
position <- "45DegPerp"

for (i in startnum:endnum)
{
  filenam <- paste(prefix, "0",sep="")
  if (i < 10) filenam <- paste(filenam, "0",sep="")
  filenam <- paste(filenam,i,exten,sep="")

  import.data(datafile,          paste("E:\\reckman\\Thesis\\Experimental
Data\\",position,"\\",energy,"\\",filenam,sep=""), "ASCII")

  trimmed <- datafile[datafile$V1 > 30 & datafile$V2 > -0.5 & datafile$V2
< 5,]

  short <- trimmed[trimmed$V1/0.05 - floor(trimmed$V1/0.05)==0,]
  Vd2.l <- loess(V2 ~ V1, short, span=0.2, degree=2, family="gaussian")

  # plot(Vd2.l)
  # points(short$V1, short$V2)

  Current.l <- loess(V3 ~ V1, short, span=0.2, degree=2,
family="gaussian")

  #plot(Current.l)
  #points(short$V1, short$V3)

  # Format of output table is: Time, Vd2, Vd2 upper error bar, Vd2 lower
error bar, Current, Current upper error bar, Current lower error bar)

  output <- cbind.data.frame(short$V1, Vd2.l$fitted.values, Vd2.l$fit +
abs(Vd2.l$residuals), Vd2.l$fit - abs(Vd2.l$residuals),
Current.l$fitted.values, Current.l$fit + abs(Current.l$residuals),
Current.l$fit - abs(Current.l$residuals))

  export.data("output",          paste("E:\\reckman\\Thesis\\Experimental
Data\\",position,"\\",energy,"\\Smoothed
Data\\sm",filenam,sep=""), "ASCII")
}

```

A.3 Triple Langmuir Probe Reduction Code

The following code was run in FORTRAN to convert the voltage and current traces to electron temperature and density measurements. It is based on the algorithm developed by Tilley [1990] and follows the outline set forth in Chapter 2.

```
Double Precision k, M, mp, mass, ne, lhs, neold, nu, neupper
Double Precision nelower
CHARACTER*32 inputfile, outputfile, tempfile
character*1 diskletter
character*3 cstartnum, cendnum, cfpos, cspos
integer startnum, endnum, num, num1, num2, num3, fpos, spos

c
c
c
c   This program solves for Te and ne from triple probe data, using
c   the formulas outlined in Tilley et al. AIAA 90-2667
c
c
c
c   Constants:
c   e = 1.609e-19
c   k = 1.381e-23

c
c   Probe exposed Area
c   A = 7.09e-6
c   Probe radius
c   rp = 1.255e-4

c
c   Mass (AMU)
c   M= 31
c   mp=1.6726e-27
c   mass (kg)
c   mass = M*mp

c
c   Guess Ti/Zi. Assume Ti = 5800K (0.5 eV), Zi = 1
c   tizi=5800

c   write(*,*) 'Triple Langmuir Probe Data Reduction Program'
c   write(*,*) 'Program takes output from S-Plus script reduce.ssc'
c   write(*,*) 'and converts Vd2 and I to Te and Ne'

c   write(*,*)
c   write(*,*) '-----'
c   write(*,*)

c
c   Prepare input file

c   write(*,*) 'Enter disk letter'
c   read(*,*) diskletter
c   write(*,*) 'Enter s-plus smoothed start record, example: ''013'''
```

```

read(*,*) cstartnum
write(*,*) 'Enter s-plus smoothed end record, example ''066'''
read(*,*) cendnum

c   Prompt for Vd3
write(*,*) 'Enter Vd3:'
read(*,*) Vd3

c   now convert startnum and endnum chars to integers for loop

num1 =ichar(cstartnum(1:1)) - 48
num2 =ichar(cstartnum(2:2)) - 48
num3 =ichar(cstartnum(3:3)) - 48

startnum = num1*100 + num2*10 + num3

num1 =ichar(cendnum(1:1)) - 48
num2 =ichar(cendnum(2:2)) - 48
num3 =ichar(cendnum(3:3)) - 48

endnum = num1*100 + num2*10 + num3

c   now we have startnum and endnum as integers, so we can do loop on
the
do 999 num = startnum,endnum

c   now we're looping on files, but we need to convert back to char
the
c   current num file we're on.

fpos = floor(real(num)/10)
spos = num - fpos*10

tempfile = diskletter//'0'//char(fpos+48)//char(spos+48)
write(*,*)tempfile

inputfile='sm'//tempfile(1:4)//'.dat'
open(1, FILE=inputfile, STATUS='OLD')

outputfile='out'//inputfile(3:10)

open(2, FILE=outputfile, STATUS='NEW')
c   Write Column Headers into Outputfile

write(2, *) 'Time,Te_smooth,Ne_smooth'

stp=0

c   Loop Over Time Steps

time=0

do while (.not.eof(1))

c   Te=40000

```

```

c
c
c   read in line from input file.
   read(1,*) garbage, time, Vd2, cur

c   ignore the first col, it is garbage

c   if voltage and current are within bounds to do analysis
   if (Vd2.gt.0.1.and.Vd2.lt.6.and.cur.gt.0.001)then
c   find Te using thin sheath approximation

do while (stp.lt.1)
    lhs=(1-exp(-e*Vd2/k/Te))/(1-exp(-e*Vd3/k/Te))
    test=abs(0.5-lhs)
    if(test.lt.0.03) then
        stp=1
    else
        Te=Te*lhs/0.5
    endif
enddo

    stp=0

c   find density using thin sheath approximation

ne=exp(0.5)*cur/A/e/sqrt(k*Te/mass)/(exp(e* Vd2/k/Te)-1)

c   If density ends up negative for some reason (bad current values)
c   set to 0

   if (ne.gt.0.1) then
       ne=ne
   else
       ne=0
   endif

   teorig=Te
   neorig=ne

c   loop until te=te

   stp3=0

c   now use these thin sheath values as input into corrected formulas
c   from Tilley

do while (stp3.lt.1)

    teold=Te
    neold=ne

c   Corrections for variation in ion current

c   find Debye Length, and various ratios

debye=69*sqrt(Te/ne)
rpdb=rp/debye
tizite=tizi/Te

```

```

c    now find paramaters for Peterson-Talbot curve fit
    alpha = 2.9/(log(rpdb) + 2.3)+0.07*(tizite)**0.75 - 0.34
    B = 1.5 + (0.85 + 0.135*(log(rpdb))**3)*tizite

c    now find Xf using Newton-Raphson method

    xf=1
    stp2 = 0

    do while (stp2.lt.1)
      xfold=xf
      eq = (B + xfold)**(2*alpha) - mass/9.11e-31*exp(-2*xfold)
      deq = 2*alpha*(B+xfold)**(2*alpha)/(B+xfold) +2*mass/9.11e-
31*
&          exp(-2*xfold)

      xf=xfold - eq/deq
      if (abs(xf-xfold).lt.1e-3) then
        stp2=1
      endif
    enddo
    stp2=0
c    Now calculate nu and beta

    nu = 2*alpha/(B+xf)
    beta = nu/k/Te*e

    if (beta.lt.0.0) then
      beta=0
    endif

c    Now find new Te

    stp4=0
    do while (stp4.lt.1)

      clhs=(1-0.5*(sqrt(1-beta*Vd2) +
&          sqrt(1+beta*(Vd3-Vd2)))*exp(-e*Vd2/
&          k/Te))/(1-exp(-e*Vd3/k/Te))
      test=abs(0.5-clhs)
c      write(*,*) test
      if (test.lt.0.003) then
        stp4=1
      else
        Te=Te*clhs/0.5
      endif
    enddo

c    Find new Ne

    Xd3=e*Vd3/k/Te
    Xd2=e*Vd2/k/Te

    ne=sqrt(6.2832)*cur/A/e/sqrt(k*Te/mass)/
&          ((B+(Xd3-Xd2)+xf)**alpha -
&          (B+xf)*exp(-(Xd3-Xd2)))

```

```

c      Convergence test on Te & ne

          if (abs(Te-teold).lt.1e-3) then
              stp3=1
          endif

          enddo
      stp=0

c
c-----
c-----
c      Output to file

          write(2, 9999) time, ',', Te/11600,',',ne,
9999          format(f6.2, A1, f6.3, A1, e13.3)

          endif

      end do

      close(1)
      close(2)
999  end do
      END

```

A.4 Peak Value Batch File

The final piece of code used is a WinBatch script that searches each data file for the maximum density and corresponding electron temperature. It then generates a report for the set of data files which contains the data file name, the maximum electron density, bulk temperature and the time that corresponds to this measurement.

```

curdir = DirGet()
StartFileNum = Askline("Start File Number", "Enter Start File Number",
"") ;Starting File Number
EndFileNum = Askline("End File Number", "Enter End File Number",
"");Ending File Number
Disk=Askline("Disk?", "What disk letter is this?","") ;Disk Letter

outhandle = FileOpen("%Disk%StartFileNum%-EndFileNum%.dat","write")

;Prepare header for this file

```

```

FileWrite(outhandle, "Record No,TimeMax,TeMax,NeMax")

For number = StartFileNum to EndFileNum

    numstr = StrCat("0", number)
    numlen = StrCharCount(numstr)
    if numlen < 3
        numstr = StrCat("0", numstr)
    endif

;Open current files up

    datafile = FileOpen("out%Disk%%numstr%.dat", "read")

;Dummy string to remove header info

    dumstr = FileRead(datafile)

    Temax=1
    nemax=1
    timemax=1

;Now loop through file

    while @TRUE

        instring=FileRead(datafile)
        if instring == "*EOF*" Then Break
        linelength = StrLen(instring)

        start=1
        count=0

        while @TRUE
            finish=StrScan(instring, ",", start, @FWDSCAN)
            if finish == 0
                Break
            else
                count=count+1
                param%count%=StrSub(instring, start, finish-
start)
                start=finish+1
                if finish == linelength then Break
                if count == 3 then Break
            endif
        endwhile

        time=param1
        Te=param2
        ne=param3

;    Display(1, "Details", "%Time% %Temax% %nemax%")

        if ne > nemax
            nemax=ne
            Temax=Te
            timemax=time
        endif
    endwhile

```

```
        if time > 60.0 then Break
    endwhile
;    now write to summary file based on this case
    FileWrite(outhandle,
StrCat("%Disk%%numstr%", "", "timemax", "", "Temax", "", "nemax"))
    FileClose(datafile)

    Beep

Next
FileClose(outhandle)

Message("Done", "%Disk%%StartFileNum% to %EndFileNum%")
```

Bibliography

- Antropov, N., Gomilka, L., Diakonov, G., Krivonosov, I., Popov, G., Orlov, M., "Parameters of Plasmoids Injected by PPT", 33rd Joint Propulsion Conference, Seattle, WA, July 6-9, 1997.
- Buften, S. A., Burton, R. L., Krier, H., "Measured Plasma Properties at the Exit Plane of a 1 kW Arcjet", 31st Joint Propulsion Conference, San Diego, CA, July 10-12, 1995.
- Burton, R. L., "Overview of US Academic Programs in Electric Propulsion", 34th Joint Propulsion Conference, Cleveland, OH, July 13-15, 1998.
- Bushman, S. S., Burton, R. L., Antonsen, E. L., "Arc Measurements and Performance Characteristics of a Coaxial Pulsed Plasma Thruster", 34th Joint Propulsion Conference, Cleveland, OH, July 13-15, 1998.
- Carter, J., Heminger, J., "Pulsed Plasma Thruster Contamination Studies", Major Qualifying Project ME-NAG-9503, Worcester Polytechnic Institute, February 1996.
- Cassidy, R. J., "Pulsed Plasma Mission Endurance Test", Air Force Space Technology Center Report, AL-TR-88-105, August 1989.
- Chen, F. F., "Electrostatic Probes" in "Plasma Diagnostic Techniques", Edited by Huddleston, R. H., and Leonard, S. L., pp. 113-199, Academic Press, 1965
- Chen, S., Sekiguchi, T., "Instantaneous Direct-Display System of Plasma Parameters by Means of a Triple Probe", Journal of Applied Physics, Vol. 36, No. 8, August 1965.
- Chen, S., "Studies of the Effect of Ion Current on Instantaneous Triple-Probe Measurements", Journal of Applied Physics, Vol. 41, No. 1, January 1971.
- Eckman, R. F., Santesson, M. T., "Pulsed Plasma Thruster Plume Diagnostics", Major Qualifying Project ME-NAG-9601, Worcester Polytechnic Institute, October 1996.
- Eckman, R. F., Gatsonis, N. A., Myers, R. M., Pencil, E. J., "Experimental Investigation of Pulsed Plasma Thruster Plume", Submitted to Journal of Propulsion and Power, 1998.

- Fife, J. M., Martinez-Sanchez, M., "Characterization of the SPT-70 Plume Using Electrostatic Probes", 34th Joint Propulsion Conference, Cleveland, OH, July 13-15, 1998.
- Gatsonis, N. A., Yin, X., "Theoretical and Computational Analysis of Pulsed Plasma Thruster Plumes", 25th International Electric Propulsion Conference, Cleveland, OH, Aug. 24-28, 1997.
- Gatsonis, N. A., Yin, X., "Hybrid (Fluid/PIC/DSMC) Simulation of Partially Ionized Jet", 21st International Symposium on Rarefied Gas Dynamics, Marseilles, Fr, July, 1998.
- Guman, W. J., Nathanson, D. M., "Pulsed Plasma Microthruster Propulsion System for Synchronous Orbit Satellite", Journal of Spacecraft and Rockets, Vol. 7, No. 4, April 1970.
- Guman, W. J., Begun, M., "Pulsed Plasma Plume Studies", Air Force Rocket Propulsion Laboratory Report, AFRPL-TR-77-2, March 1977.
- Guman, W. J., Begun, M., "Exhaust Plume Studies of a Pulsed Plasma Thruster", 13th International Electric Propulsion Conference, San Diego, CA, Apr. 25-27, 1978.
- Habiger, H. A., Auweter-Kurtz, M., "Investigation of an High Enthalpy Air Plasma Flow with Electrostatic Probes", 31st AIAA Thermophysics Conference, New Orleans, LA, June 17-20, 1996.
- Hirata, M., Murakami H., "Exhaust Gas Analysis of a Pulsed Plasma Engine", IEPC 84-52, International Electric Propulsion Conference, Tokyo, Japan, 1984.
- MathSoft, "S-Plus 4 Guide to Statistics", Mathsoft Inc., Seattle, WA, July 1997.
- Markusic, T. E., Spores, R. A., "Spectroscopic Emission Measurements of a Pulsed Plasma Thruster Plume", 33rd Joint Propulsion Conference, Seattle, WA, July 6-9, 1997.
- McGuire, M. L., Myers, R. M., "Pulsed Plasma Thrusters for Small Spacecraft Attitude Control", 1996.
- Myers, R. M., Oleson, S. R., Curran, F. M., Schneider, S. J., "Small Satellite Propulsion Options", 29th Intersociety Energy Conversion Engineering Conference, Monterey, CA, Aug. 7-11, 1994; p. 744-749.
- Myers, R. M., Oleson, S. R., McGuire, M., Meckel, N. J., Cassady, R. J., "Pulsed Plasma Thruster Technology for Small Satellite Missions", NASA CR-198427 November 1995.

- Myers, R. M., Arrington, L. A., Pencil, E. J., Carter, J., Heminger, J., Gatsonis, N., "Pulsed Plasma Thruster Contamination", 32nd Joint Propulsion Conference, Lake Buena Vista, FL, July 1-3, 1996.
- Papini, D. A., Slade, T. R., "Pulsed Plasma Thruster Plume Investigation", Major Qualifying Project ME-NAG-9701, Worcester Polytechnic Institute, May 1997.
- Pencil, E. J., Personal Communication, November, 1998.
- Pollard, J. E., Jackson, D. E., Marvin, D. C., Jenkin, A. B., Janson, S. W., "Electric Propulsion Flight Experience and Technology Readiness", 29th Joint Propulsion Conference and Exhibit, Monterey, CA, June 28-30, 1993.
- Spanjers, G. G., Malak, J. B., Leiweke, R. L., Spores, R. A., "The Effect of Propellant Temperature on Efficiency in the Pulsed Plasma Thruster", 33rd Joint Propulsion Conference, Seattle, WA, July 6-9, 1997.
- Spanjers, G. G., Lotspeich, J. A., Spores, R. A., "Propellant Losses Because of Particulate Emission in a Pulsed Plasma Thruster", Journal of Propulsion and Power, Vol. 14, No. 4, July, 1998.
- Thomassen, K. I., Vondra, R. J., "Exhaust Velocity Studies of a Solid Teflon Pulsed Plasma Thruster", Journal of Spacecraft and Rockets, Vol. 9, No. 1, January 1972.
- Thomassen, K. I., Tong, D., "Interferometric Density Measurements in the Arc of a Pulsed Plasma Thruster", Journal of Spacecraft and Rockets, Vol. 10, No. 3, March 1973.
- Thomassen, K. I., "Radiation from Pulsed Electric Thrusters", Journal of Spacecraft and Rockets, Vol. 10, No. 10, October 1973.
- Tilley, D. L., Kelly, A. J., Jahn, R. G., "The Application of the Triple Probe Method to MPD Thruster Plumes", 21st International Electric Propulsion Conference, Orlando, FL, July 18-20, 1990.
- Turchi, P. J., Mikellides, P. G., "Modeling of Ablation-Fed Pulsed Plasma Thrusters", 31st Joint Propulsion Conference, San Diego, CA, July 10-12, 1995.
- Turchi, P. J., "Directions for Improving PPT Performance", 25th International Electric Propulsion Conference, Cleveland, OH, August 24-28, 1997.
- Turchi, P. J., Mikellides, I. G., Mikellides, P. G., "Theoretical Investigation of Pulsed Plasma Thrusters", 34th Joint Propulsion Conference, Cleveland, OH, July 13-15, 1998.

Vondra, R. J., Thomassen, K. I., Solbes, A., “Analysis of Solid Teflon Pulsed Plasma Thruster”, Journal of Spacecraft and Rockets, Vol. 7, No. 12., December 1970.

Vondra, R. J., Thomassen, K. I., “Flight Qualified Pulsed Electric Thruster for Satellite Control”, Journal of Spacecraft and Rockets, Vol. 11, No. 9, September 1974.

Yin, X., Gatsonis, N. A., “Numerical Investigation of Pulsed Plasma Thruster Plumes”, 25th International Electric Propulsion Conference, Cleveland, OH, Aug. 24-28, 1997.

Ziemer, J. K., Cubbin, E. A., Choueiri, E. Y., Birx, D., “Performance Characterization Of A High Efficiency Gas-Fed Pulsed Plasma Thruster”, 33rd Joint Propulsion Conference, Seattle, WA, July 6-9, 1997.